THE JOURNAL OF BIOLOGICAL CHEMISTRY VOL. 281, NO. 16, pp. 11332–11346, April 21, 2006

Inhibition of Heme Oxygenase-1 Interferes with the Transforming Activity of the Kaposi Sarcoma Herpesvirus-encoded G Protein-coupled Receptor*◆

Received for publication, November 14, 2005, and in revised form, February 1, 2006 Published, JBC Papers in Press, February 13, 2006, DOI 10.1074/jbc.M512199200

Maria Julia Marinissen[‡1], **Tamara Tanos**[§2], **Marta Bolós**[‡], **Maria Rosa de Sagarra**[‡], **Omar A. Coso**[§], **and Antonio Cuadrado**[‡]

From the [‡]*Instituto de Investigaciones Biomédicas A. Sols Universidad Autónoma de Madrid-Consejo Superior de Investigaciones Científicas, Departamento de Bioquímica, Facultad de Medicina, Universidad Autónoma de Madrid, Madrid 28029, Spain and the* [§]*Departamento de Fisiología, Biología Molecular y Celular, Facultad de Ciencias Exactas y Naturales, Universidad de Buenos Aires, Instituto de Fisiologia, Biologia Molecular and Neurociencias-Consejo Nacional de Investigaciones Científicas y Técnicas, 1428 Buenos Aires, Argentina*

Heme oxygenase-1 (HO-1), the inducible enzyme responsible for the rate-limiting step in the heme catabolism, is expressed in AIDS-Kaposi sarcoma (KS) lesions. Its expression is up-regulated by the Kaposi sarcoma-associated herpesvirus (KSHV) in endothelial cells, but the mechanisms underlying KSHV-induced HO-1 expression are still unknown. In this study we investigated whether the oncogenic G protein-coupled receptor (KSHV-GPCR or vGPCR), one of the key KSHV genes involved in KS development, activated HO-1 expression. Here we show that vGPCR induces HO-1 mRNA and protein levels in fibroblasts and endothelial cells. Moreover, targeted knock-down gene expression of HO-1 by small hairpin RNA and chemical inhibition of HO-1 enzymatic activity by tin protoporphyrin IX (SnPP), impaired vGPCR-induced survival, proliferation, transformation, and vascular endothelial growth factor (VEGF)-A expression. vGPCR-expressing cells implanted in the dorsal flank of nude mice developed tumors with elevated HO-1 expression and activity. Chronic administration of SnPP to the implanted mice, under conditions that effectively blocked HO-1 activity and VEGF-A expression in the transplanted cells, strikingly reduced tumor growth, without apparent side effects. On the contrary, administration of the HO-1 inducer cobalt protoporphyrin (CoPP) further enhanced vGPCR-induced tumor growth. These data postulate HO-1 as an important mediator of vGPCR-induced tumor growth and suggest that inhibition of intratumoral HO-1 activity by SnPP may be a potential therapeutic strategy.

Heme oxygenase (HO)[3] proteins control heme metabolism and iron levels by catalyzing the degradation of the heme group (iron protoporphyrin IX). Oxidative cleavage of the protoporphyrin ring results in formation of the physiological messenger molecule carbon monoxide (CO), free iron, and biliverdin, the latter being subsequently reduced to the antioxidant bilirubin by cytosolic biliverdin reductase (1). So far, three mammalian isoforms of heme oxygenase have been identified: HO-1, HO-2, and HO-3. HO-2 is a constitutive 36-kDa isoform present mostly in brain and testis, and HO-3 has been recently cloned but its role remains uncertain because of its very low enzyme activity compared with that of the other variants (1). In contrast, HO-1 is an inducible and ubiquitous 32-kDa isoform highly expressed in spleen and liver and normally found in very low levels in most mammalian tissues (1). The regulation of its potent enzymatic activity depends primarily on the control of HO-1 expression at the transcriptional level (1–3). Because of the antioxidant properties of the heme metabolism products, HO-1 is considered a cytoprotector molecule involved in several physiological responses against oxidative and cellular stress (2). Its expression is triggered by stress-inducing stimuli including hypoxia, heavy metals, UV radiation, reactive oxygen species, nitric oxide (NO), antioxidants, growth factors, and hormones (4–8). HO-1 prevents a wide range of stress and inflammatory responses such as endotoxic shock, ischemia/reperfusion injury, and hyperoxia-induced lung injury among others (9–11). In addition, evidence for the cytoprotective role of HO-1 derives from organ transplantation research, in which the expression of HO-1 by the graft vasculature is key for heart, liver, kidney, thyroid, and pancreatic islet allografts survival (11).

An increasing number of studies support the notion of an important role for HO-1 in the physiology of the vasculature, where by means of the heme degradation by-products, it protects endothelial cells from a wide variety of apoptotic stimuli (3). Indeed, HO-1 has been recently defined as an important regulator of endothelial cell cycle control, proliferation, vascular endothelial growth factor (VEGF) secretion, and angiogenesis (3). As such, angiogenic stimulating factors including interleukins 1 and 6 (IL-1 and IL-6), transforming growth factor β, prolactin, 15-deoxy-Δ12,14-prostaglandin J (2), and atrial natriuretic peptide are able to up-regulate HO-1 expression (3). Interestingly, a recent study has shown that HO-1 expression and activity are induced by an angiogenic oncovirus, the Kaposi sarcoma-associated herpesvirus (KSHV), in endothelial cells. Besides, elevated levels of the enzyme are detectable in biopsy tissue from oral AIDS-Kaposi sarcoma lesions (12).

* This work was supported in part by grants from Fundación Médica Mutua Madrileña (Spain), Grant SAF2005-03020 from Ministerio de Educación y Ciencia (Spain), Centro de Estudios de América Latina (Universidad Autónoma de Madrid-Banco Santander, Spain) and RSMN (03/08) from the Health Institute Carlos III. The costs of publication of this article were defrayed in part by the payment of page charges. This article must therefore be hereby marked "*advertisement*" in accordance with 18 U.S.C. Section 1734 solely to indicate this fact.

◆ This article was selected as a Paper of the Week.

[1] To whom correspondence should be addressed: Inst. de Investigaciones Biomédicas A. Sols UAM-CSIC, Dept. de Bioquímica, Facultad de Medicina, Universidad Autónoma de Madrid, Laboratorio C-11, Arzobispo Morcillo 4, Madrid 28029, Spain. Tel.: 34-91-497-5464; Fax: 34-91-576-7442; E-mail: mjmarinissen@iib.uam.es.

[2] Recipient of European Molecular Biology Organization and International Union against Cancer International Cancer Technology Transfer fellowships during periods spent at the laboratory in Spain.

[3] The abbreviations used are: HO, heme oxygenase; VEGF, vascular endothelial growth factor; IL, interleukin; KSHV, Kaposi sarcoma-associated herpesvirus; GPCR, G protein-coupled receptor; HA, hemagglutinin; shRNA, small hairpin RNA; DMEM, Dulbecco's modified Eagle's medium; SVEC, simian virus 40, large T-antigen-immortalized, murine endothelial cell; CoPP, cobalt protoporphyrin; SnPP, tin protoporphyrin IX; ZnPP, zinc protoporphyrin; PBS, phosphate-buffered saline; GAPDH, glyceraldehyde-3-phosphate dehydrogenase; PDI, protein-disulfide isomerase; DAPI, 4′,6-diamidino-2-phenylindole; 7-AAD, 7-aminoactinomycin D; RT, reverse transcription; GFP, green fluorescent protein.

The Kaposi sarcoma (KS) is the most frequent tumor in AIDS patients, characterized by multifocal angioproliferative lesions containing spindle cells derived from the infection of endothelial cells by the KSHV (13). This virus (also denominated human herpesvirus-8) is involved in all clinical forms of KS. Its genome harbors KSHV unique genes, common genes shared with other herpesviruses, and genes with homology to mammalian signal transduction proteins (14). One gene from the latter group, the open reading frame 74, encodes a G protein-coupled receptor (GPCR) named KSHV-GPCR or vGPCR, which is related to the mammalian IL-8 receptor CXCR2 (15). This receptor has an $Asp^{142} \rightarrow Val$ mutation in a highly conserved Asp-Arg-Lys (DRY) sequence in homologue mammalian GPCRs, which enables its constitutive, ligand-independent activity. Thus, vGPCR is able *per se* to induce transformation in fibroblasts, angiogenesis in endothelial cells (16), and human KS-resembling angioproliferative lesions (16–18). Recent distinct experimental strategies using animal models revealed that vGPCR has a key role in the development of KS. Despite the fact that only few cells in KS-like lesions are vGPCR-positive (18), down-regulation of its expression results in diminished expression of angiogenic factors and tumor regression (19), which confirms the key role of vGPCR in KS-induced oncogenesis.

Taking into account the predominant function of vGPCR in KS and the elevated expression of HO-1 observed in KS lesions and KS-infected endothelial cells, the goal of this study was to investigate whether vGPCR could induce HO-1 expression and if so to explore the putative role of the enzyme in vGPCR-dependent transformation. Accordingly, we show that the viral oncogene induced HO-1 mRNA and protein levels and that HO-1 was highly expressed in mouse tumors derived from vGPCR-transfected cells. Our data indicate that targeted knockdown gene expression of HO-1 and chemical inhibition of HO-1 enzymatic activity impaired vGPCR-induced VEGF expression, survival, proliferation, and transformation both in cell culture and in a murine allograft tumor model. These findings uncovered the identity of HO-1 as a potential therapeutic target in KS.

EXPERIMENTAL PROCEDURES

DNA Constructs—The plasmid pHO-1-Luc was provided by J. Alam and contains a 15-kb murine HO-1 promoter upstream of a luciferase gene as described previously (5). The pVEGF-Luc was a kind gift from B. Vonderhaar and R. Hovey (20). pCEFL-AU5-vGPCR, pCEFL-VEGF, pCEFL-β-galactosidase, pCEFL-GFP, and pCEFL-AU5 Ras V12 have been described previously (18, 21). The murine full-length HO-1 was amplified by RT-PCR from RNA from hemin-treated NIH3T3 cells with the primers 5′-GCGAATTCACCATGGAGCGTCCACAGCCCGACAG and 3′-GCGCGGCCGCTTACATGGCATAAATTCCCACTG and subcloned into an HA-tagged pCEFL expression vector as an EcoRI/NotI fragment. pCEP4, a plasmid carrying a hygromycin resistance gene, was commercially purchased (Invitrogen, Barcelona, Spain). pS-shRNAHO-1, a plasmid carrying shRNA for HO-1, was engineered by annealing the single strand oligonucleotides 5′-GATCCCCAACTTTCAGAAGGGCCAGGTGTTCAAGAGACACCTGGCCCTTCTGAAAGTTTTTTTGGAAA and 3′-GGGTTGAAAGTCTTCCCGGTCCACAAGTTCTCTGTGGACCGGGAAGACTTTCAAAAAAACCTTTTCGA and inserting the double strand oligonucleotide in the pSilencer 1.0-U6 plasmid (Ambion).

Cell Lines and Transfections—NIH3T3 fibroblasts were maintained in Dulbecco's modified Eagle's medium (DMEM) (Invitrogen) supplemented with 10% calf serum. Simian virus 40, large T-antigen-immortalized, murine endothelial cells (SVECs) were maintained in DMEM supplemented with 10% fetal bovine serum. Stable transfections were performed using the calcium phosphate technique (22). NIH3T3 and SVEC cells were plated at 20% confluence in 10-cm plates and transfected with 10 μg of pCEFL, pCEFL-vGPCR, or pCEFL-HA-HO-1. Transfected cells were selected with 750 μg/ml G418 (Promega Corp., Madrid, Spain). NIH-vGPCR cells were further transfected with 100 ng of pCEP4 along with 10 μg of pSilencer (Ambion) (NIH-$vGPCR_{shRNA}$), pS-shRNAHO-1 (NIH-$vGPCR_{shRNAHO\text{-}1}$), or pCEFL-VEGF (NIH-vGPCR-VEGF). Transfected cells were selected with 160 μg/ml hygromycin B from *Streptomyces* (Sigma, Madrid, Spain). Transient transfections were performed using the Lipofectamine Plus Reagent (Invitrogen).

Analysis of mRNA Levels by Semiquantitative Reverse Transcription-PCR—Cells were treated for 6 h with vehicle (control), 100 ng/ml IL-6, 250 μM $CoCl_2$, 150 ng/ml IL-8 or GROα (Sigma), and 10 μM cobalt protoporphyrin (CoPP) (Frontier Scientific Europe Ltd., Great Britain). When indicated, cells were preincubated with 50–100 μM tin protoporphyrin IX (SnPP) (Frontier Scientific Europe Ltd.) for 24–48 h. Total RNA from cells and tumors was extracted by homogenization in TRIzol (Invitrogen). Briefly, cells were grown to 80% confluence, serum-starved for 24–48 h, washed with cold PBS, and lysed in TRIzol according to the manufacturer's indications. Total RNA from tumors was obtained by homogenizing the tissue in TRIzol with a Teflon homogenizer. Equal amounts of RNA (1 μg) were reverse-transcribed to obtain cDNA with the transcription first strand cDNA kit (Roche Diagnostics GmbH, Madrid, Spain). PCRs were performed using the Ready Mix RedTaq PCR reactive mix (Sigma). The nucleotide sequences HO-1 5′-CAACAGTGGCAGTGGGAATTT and HO-1 3′-CCAGGCAAGATTCTCCCTTAC were used to amplify a 106-bp HO-1 fragment. To obtain a 1029-bp vGPCR fragment, the primers were 5′-GCGAATTCACCATGGCGGCCGAGGATTTCCTAAC, vGPCR 3′-GCGCGGCCGCCTACGTGGTGGCGCCGGACATGA. The three splice variants of VEGF-A were amplified using VEGF-A 5′-CTGCTCTCTTGGGTGCACTGG and VEGF-A 3′-ACCGCCTTGGCTTGTCACAT primers. Expected product sizes were 431, 563, and 635 bp corresponding to the VEGF120, VEGF164, and VEGF188 splice variant isoforms (20); VEGF-C 5′-TGAACACCAGCACAGGTTAC and VEGF-C 3′-TCTTGTTAGCTGCCTGACAC oligonucleotides yielded a VEGF C fragment of 204 bp. A fragment of 102 bp from the glyceraldehyde-3-phosphate dehydrogenase (GAPDH) housekeeping gene was amplified in parallel to all reactions to ensure that equal amounts of starting cDNA were used in each reaction. The nucleotide sequences of the corresponding primers were GAPDH 5′-TCCATCACAACTTTGGCATTG and GAPDH 3′-TCACGCACAAGCTTTCCA. After an initial denaturalization step of 2 min at 94 °C, amplification of each cDNA was performed in 22–34 cycles (in increments of 2) to detect the linear amplification phase. Most reactions were set at 28 cycles, which also allowed detection of basal HO-1 mRNA levels in control cells. The same amount of cycles were used for VEGF-A, VEGF-C, and GAPDH using a thermal profile of 30 s at 94 °C, 30 s at 58 °C, and 30 s at 72 °C. For full-length mouse HO-1 and vGPCR, the amplifications were performed with 30 cycles of 1 min at 94 °C, 1 min at 58 °C, and 1 min at 72 °C. The PCR products were detected by electrophoresis in agarose gels and fluorescence under UV light upon ethidium bromide staining.

Luciferase Reporter Assays—Cells were transfected with different expression plasmids together with 0.1 μg of the indicated reporter plasmid and 100 ng of p*Renilla*-null (Promega Corp.) per well in 6-well plates. In all cases, the total amount of plasmid DNA was adjusted with pcDNA3-β-galactosidase. When indicated, cells were pretreated for 24 h with vehicle or 50–100 μM SnPP (Frontier Scientific Europe Ltd.) dissolved in Me_2SO, 50 nM bilirubin, or 1 μM $[Ru(CO)_3Cl_2]_2$ (Sigma).

Firefly and *Renilla* luciferase activities present in cellular lysates were assayed using the dual luciferase reporter system (Promega Corp.), and light emission was quantified using a BG1 Optocomp I, GEM Biomedical luminometer (Sparks, NV).

Western Blot—HA-HO1 and GFP-HO-1 were detected by Western blotting with anti-HA and anti-GFP monoclonal antibodies (HA.11, Covance, Inc. and Clontech, respectively). Endogenous HO-1 and HO-2 from cell lysates and tumor microsomes were detected by rabbit and mouse monoclonal specific antibodies (StressGen Biotechnologies). Protein-disulfide isomerase (PDI) was detected with a specific anti PDI rabbit antibody (4). Proteins were visualized by enhanced chemiluminescence detection (Amersham Biosciences) using goat anti-mouse and anti-rabbit IgGs coupled to horseradish peroxidase as the secondary antibody (Amersham Biosciences).

Indirect Immunofluorescence—NIH3T3 cells were seeded on glass coverslips and transfected by Lipofectamine Plus reagents (Invitrogen). Cells were serum-starved for 24 h, washed twice with 1× PBS, and then fixed and permeabilized with 4% formaldehyde and 0.05% Triton X-100 in 1× PBS for 10 min. After washing with PBS, cells were blocked with 1% bovine serum albumin and incubated with anti HO-1 (StressGen Biotechnologies), anti-AU5, or anti-HA antibodies (Covance, Inc.) as primary antibodies for 1 h. Following incubation, cells were washed three times with 1× PBS and then incubated for an additional hour with the corresponding secondary antibodies (1:200) conjugated with tetramethylrhodamine B isothiocyanate and fluorescein isothiocyanate (Molecular Probes). Cells were washed three times with 1× PBS and stained with DAPI (1 μg/ml) (Molecular Probes) in the last wash. Coverslips were mounted in Fluorosafe mounting medium (Calbiochem) and viewed using a Nikon Eclipse TE2000-S photomicroscope equipped with epifluorescence.

Immunohistochemistry—Tumor, skin, and liver tissues were removed and fixed in 4% paraformaldehyde in 1× PBS, transferred to 70% ethanol, and embedded in paraffin. Sections were hydrated in a graded xylene/ethanol series. Antigens were retrieved by heat, and sections were incubated with the anti HO-1 antibody (StressGen Biotechnologies) (1:500). The antibody was recognized by labeled polymer-AP (DakoCytomation) and alkaline phosphatase activity was developed using Fast Red (DakoCytomation). Slides were also stained with hematoxylin, dehydrated, and mounted in Glycergel mounting medium (DakoCytomation).

Focus-forming Assays—NIH3T3 cells were transfected by the calcium-phosphate precipitation technique with different indicated expression plasmids as described previously (22). The day after transfection, cells were washed three times with DMEM and kept in DMEM supplemented with 5% calf serum alone or with 50–100 mM SnPP for 2–3 weeks until *foci* were scored. Alternatively, 5×10^4 NIH-vGPCR, NIH-vGPCR$_{shRNA}$, or NIH-vGPCRsh$_{RNAHO-1}$ cells were seeded on a 50% confluent monolayer of NIH3T3 cells and cultured as above until foci were detected. Cells were fixed with methanol for 20 min, washed with water, dried, and stained with Giemsa (Sigma).

Measurement of HO Activity in Tumors—HO activity in microsomes from solid tumors or livers of control and SnPP-treated mice was assayed following the protocol described previously (23). Briefly, tumors and livers were homogenized by a Polytron homogenizer in ice-cold homogenization buffer (30 mM Tris-HCl, pH 7.5, 0.25 M sucrose, 0.15 M NaCl, 10 μg/ml leupeptin, 10 μg/ml trypsin inhibitor, 2 μg/ml aprotinin, and 1 mM phenylmethylsulfonyl fluoride). After brief sonication, lysates were centrifuged at 10,000 × *g* for 15 min at 4 °C and supernatants ultracentrifuged at 100,000 × *g* for 1 h at 4 °C. Microsomal fractions were resuspended in 1 ml of 100 mM potassium phosphate buffer, pH 7.4, containing 2 mM $MgCl_2$. Protein concentration was determined using a small aliquot of these suspensions (Bio-Rad). The HO-1 activity assay was carried out by mixing microsome proteins (1 mg), cytosol fraction of rat liver as a source of biliverdin reductase (2 mg), 100 mM potassium phosphate buffer, pH 7.4, containing 2 mM $MgCl_2$, 10 μM hemin, 2 mM glucose-6-phosphate, 0.2 unit of glucose-6-phosphate dehydrogenase, and 0.8 mM NADPH. All chemical reagents were commercially obtained (Sigma). The reaction was conducted in the dark for 1h at 37 °C and terminated by the addition of 1 ml chloroform (Sigma). The amount of extracted bilirubin was calculated by the difference in absorption between 464 and 530 nm using an extinction coefficient of 40 mM^{-1} cm^{-1} for bilirubin.

In Vitro Apoptosis Assay—Apoptosis was determined by staining cells with the annexin V-PE apoptosis detection kit (BD Biosciences). Briefly, cells were plated in 6-well plates (250,000 cells/well), serum-starved for 48 h, and simultaneously treated with vehicle or 100 μM SnPP in Me_2SO. Attached cells were harvested and stained with annexin V-PE as a marker for early apoptosis, and 7-AAD, a vital dye, for 15 min in the dark. The number of apoptotic cells was determined by flow cytometry (FACSVantage SE with Digital DiVa, BD Biosciences).

Cell Proliferation and [^{3}H]Thymidine Incorporation—Cells were seeded in 24-well plates, at 100,000 cells per well. After overnight growth, the cells were serum-starved for 48 or 96 h, harvested, and counted in a New Bauer chamber. Alternatively, after 48-h serum starvation, cells were incubated with [^{3}H]thymidine (PerkinElmer Life Sciences) for 2 h. Monolayers were washed 3 times with PBS, twice with 5% trichloroacetic acid, and lysed in 1 N NaOH. Aliquots were counted by liquid scintillation, and parallel protein samples were quantified (Bio-Rad) for normalization.

Tumor Allografts in Athymic Nude Mice and Antitumor Effect of SnPP—SVEC, NIH, SVEC-vGPCR, NIH-vGPCR, NIH-vGPCR$_{shRNA}$, and NIH-vGPCR$_{shRNAHO-1}$ stable cell lines were used to induce tumor allografts in 7-week athymic (*nu/nu*) nude female mice. Cells were harvested, washed, counted, and resuspended in PBS. 1×10^6 viable cells were transplanted subcutaneously into the right flank of the mouse. Mice were monitored twice weekly until each animal developed one tumor in the area of the cell injection. Tumors were noticeable and reached a diameter of ~3 mm 20 days after cell injection. At this point, mice were separated in groups of five animals and were treated with vehicle (control), SnPP, or CoPP (10 μmol/kg of body weight dissolved in 0.1 N NaOH in PBS, pH 7.5) administered subcutaneously in the right flank daily for the indicated times. Tumor volume and body weight were measured every other day during the period of investigation. Tumor volumes (V) were determined by the formula $V = L \times W^2 \times 0.5$, with L being the longest cross-section and W the shortest.

Statistical Analysis—Data are shown as mean ± S.E. Statistical difference of tumor volumes was calculated by the two-tailed impaired t test. A p value <0.05 (*) was considered statistically significant.

Image Analysis and Quantification—Different band intensities corresponding to ethidium bromide detection of DNA samples or Western blot detection of protein samples were quantified using the Scion Image program.

RESULTS

Transient Expression of vGPCR from the Kaposi Sarcoma-associated Herpesvirus Induces ho-1 Promoter Activity and HO-1 Protein Expression—As one of the first observations of the transforming activity of vGPCR derived from its overexpression in NIH3T3 fibroblasts (16), we used this cell line to investigate whether the receptor was able to induce the transcriptional activity of a 15-kb murine *ho-1* promoter

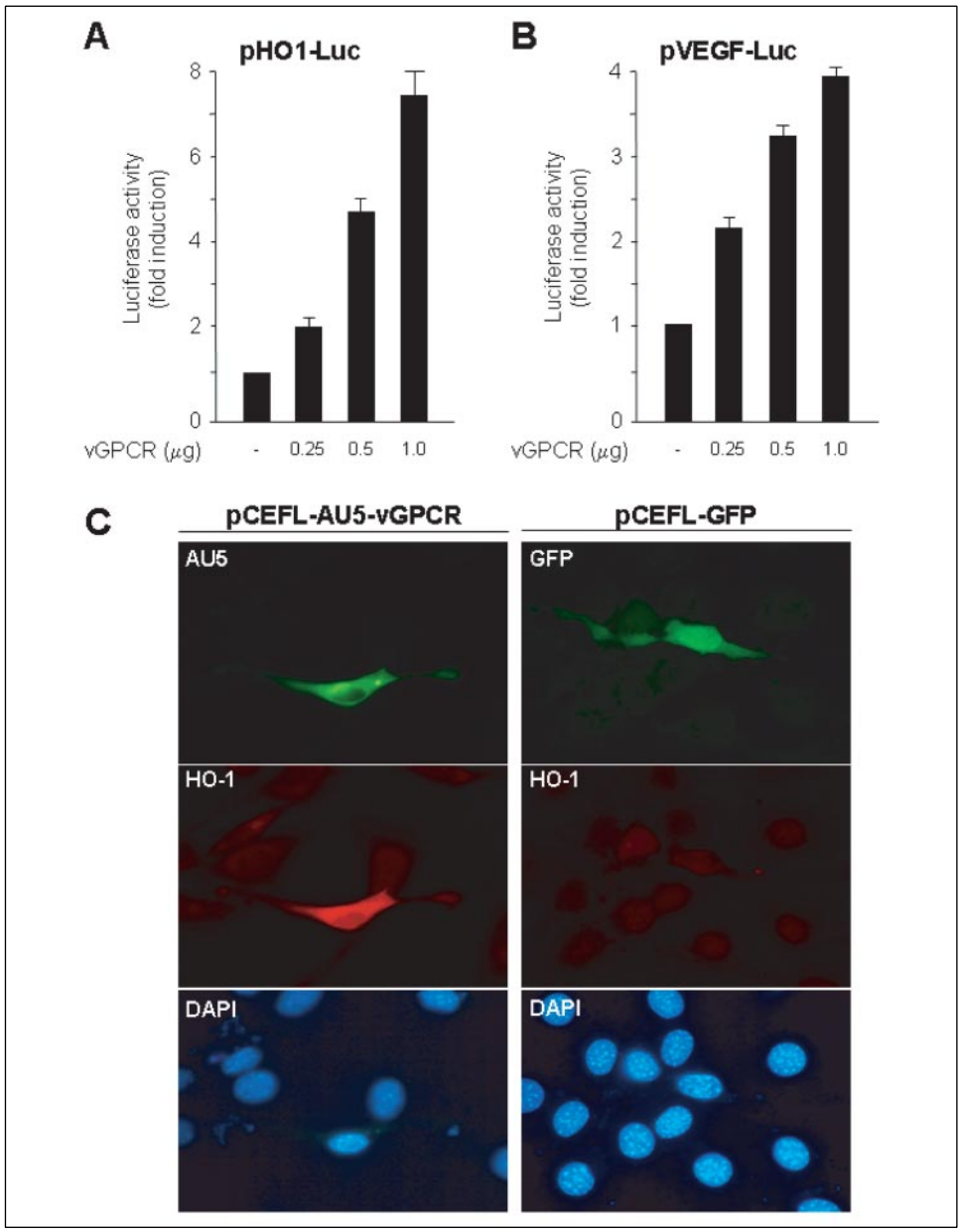

FIGURE 1. **vGPCR induces *ho-1* promoter activity and HO-1 expression.** *A* and *B*, NIH3T3 cells were cotransfected with 10 ng of pHO1-Luc or 25 ng of pVEGF-Luc along with 100 ng of p*Renilla*-Luc and different amounts of pCEFL-vGPCR per well, as indicated. The total amount of plasmid DNA in each transfection was equally adjusted with pcDNA3-β-galactosidase. 24 h after transfection and serum starvation, lysates were assayed for *Firefly* and *Renilla* luciferase activities. The data represent average *Firefly* luciferase activity normalized by *Renilla* luciferase activity in each sample ± S.E. from triplicates expressed as fold induction relative to control (−) from a typical experiment. Similar results were obtained in three additional experiments. *C*, cells were seeded on coverslips, transfected with pCEFL-AU5-vGPCR or pCEFL-GFP serum-starved, and analyzed by immunofluorescence for HO-1 expression with an anti-HO-1 antibody, GFP, and nuclear staining with DAPI. The pictures are representative of 20–30 different fields.

cloned upstream of the luciferase reporter gene (pHO1-Luc). Indeed, vGPCR activated pHO1-Luc in a dose-dependent manner in a range between 2- and 6-fold, as shown in Fig. 1*A*. The effect of vGPCR on the *ho-1* promoter activity was comparable with that of the receptor on the activity of a reporter gene driven by the vascular endothelial growth factor (*vegf*) promoter (pVEGF-Luc), a known target DNA regulatory sequence for the viral receptor (16), which served as a control (Fig. 1*B*). vGPCR, unlike its cellular homologue CXCR2, has ligand-independent activity. It has an Asp142 → Val mutation in a highly conserved Asp-Arg-Lys (DRY) sequence that enables it constitutive ligand-independent activity and its capacity to induce foci, tumors, and VEGF secretion (16, 24). Although some initial reports indicate that vGPCR can be further activated by IL-8 or GROa (25)), in our model, the addition of neither of these two factors to vGPCR-transfected cells induced a further increase in pHO-1 or pVEGF-Luc activity (data not shown), indicating that the constitutive activity of the receptor *per se* induces HO-1 expression.

To investigate whether the effect of the transient transfection of the viral receptor on the ectopic *ho-1* promoter was indicative of its effect on the expression of the endogenous HO-1 protein, we carried out immunofluorescence studies. As expected, overexpression of an AU5-tagged form of vGPCR (pCEFL-AU5-vGPCR) induced the expression of HO-1, as only cells stained positive for the AU5 antibody resulted in positive staining when incubated with a specific HO-1 antibody (Fig. 1*C*, *left panels*). As a control, we transfected cells with a pCEFL-GFP plasmid and incubated them with the HO-1 antibody. As shown in Fig. 1*C*, *right panels*, cells overexpressing GFP did not show HO-1-positive staining. These results show that transient expression of vGPCR induced both *ho-1* promoter activity and endogenous HO-1 protein expression.

Stable Transfection of vGPCR Increases HO-1 mRNA and Protein Levels—To evaluate the effect of constitutive, prolonged expression of vGPCR on HO-1 levels, we stably transfected NIH3T3 cells with empty vector (pCEFL) or an expression vector carrying a cDNA for full-length

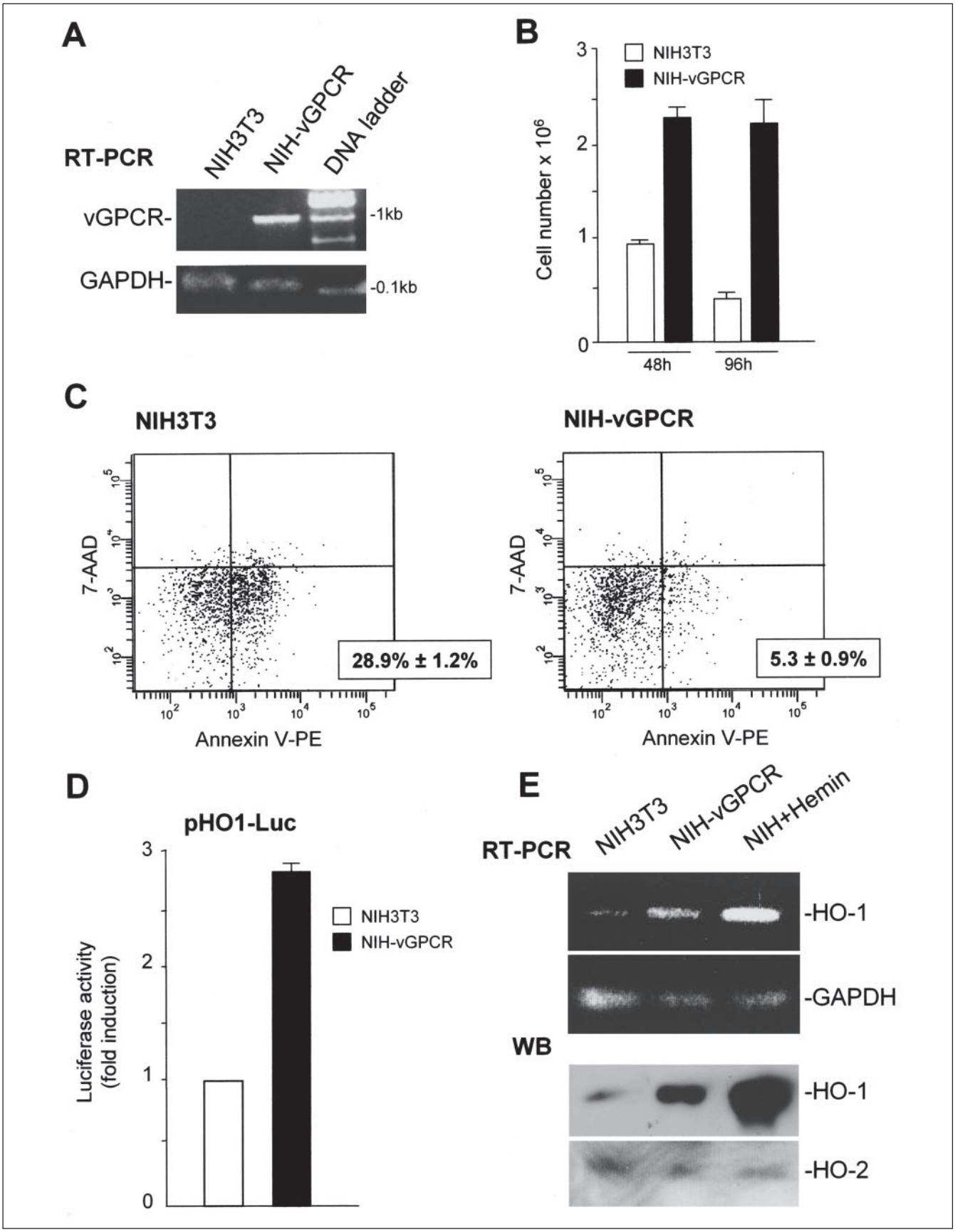

FIGURE 2. **Constitutive expression of vGPCR increases HO-1 mRNA and protein levels in NIH3T3 cells.** *A*, NIH3T3 and NIH-vGPCR cells were serum-starved for 24 h and total RNA isolated. vGPCR and GAPDH levels were detected by RT-PCR. Products were visualized by ethidium bromide staining. *B*, equal number of NIH3T3 and NIHvGPCR cells were plated and serum-starved after 24 h in culture. 48 and 96 h after serum starvation, cells were harvested and counted in a Neubauer chamber. *C*, cells were cultured as above, and after 48-h serum

wild-type vGPCR (pCEFL-vGPCR). After antibiotic selection and several further passages, only NIH-vGPCR cells expressed the viral oncogene, in contrast to NIH3T3 cells, as judged by RT-PCR detection with specific primers (Fig. 2*A*). To ensure that equal amounts of template RNA were used in the preparation of cDNA, detection of the constitutive GAPDH gene was used as a control (Fig. 2*A*, *lower gel*). To characterize the NIH-vGPCR cell population, we compared its cell number with that of NIH3T3 cells at different time points after serum withdrawal. After 48 h serum-starvation, NIH-vGPCR cells doubled their number with respect to normal fibroblasts (Fig. 2*B*). After 96 h, the number of NIH3T3 cells dropped significantly, whereas the number of NIH-vGPCR cells remained steady indicating that most likely survival, antiapoptotic mechanisms triggered by the oncogene were in place. Indeed, after 48 h of serum starvation, 28.9% cells from the NIH3T3 population presented signs of early apoptosis as indicated by the positive staining with annexin V-PE (Fig. 2*C*, *left panel*, *lower right quadrant*), whereas only a 5.3% of the NIH-vGPCR cells were apoptotic (Fig. 2*C*, *right panel*, *lower right quadrant*). To verify the transformed phenotype that NIH-vGPCR cells acquire after several passages (16), we plated 5×10^5 cells onto a monolayer of NIH3T3, and as expected, foci appeared after 2–3 weeks (data not shown). Once confirmed the vGPCR growth-promoting effect on our cell model, we measured the transcriptional activity of pHO1-Luc in both cell types. As shown Fig. 2*D*, the activity of the reporter plasmid was increased ~2.5-fold in NIH-vGPCR when compared with NIH3T3. Similar results were obtained with pVEGF-Luc used as a positive control (data not shown). To assess endogenous HO-1 mRNA and protein expression levels, we performed semiquantitative RT-PCR and Western blot experiments. We found that whereas NIH3T3 cells expressed very low levels of HO-1, the mRNA levels of the enzyme were induced in NIH-vGPCR cells by 4.2-fold. HO-1 from hemin-treated NIH3T3 was assayed as a positive control (2). Constitutive expression of vGPCR induced specifically HO-1 mRNA levels, as GAPDH did not change (Fig. 2*E*, *upper panels*). Under these conditions, the mRNA expression of the constitutive, non-inducible HO-2 isoform was very low and steady (data not shown). Increased HO-1 mRNA levels correlated directly with changes in protein levels. As shown in Fig. 2*E* (*lower panels*), the result of Western blot experiments paralleled mRNA analysis, as HO-1 was increased by 5.1-fold in NIH-vGPCR with respect to NIH3T3. As a protein loading control, we studied HO-2 levels, and as above, we found that it was very poorly expressed and unaltered in both NIH3T3 and NIH-vGPCR cells. Together, these results corroborate that the activity of the *ho-1* promoter and HO-1 protein expression were induced after both a short, transient overexpression of vGPCR and in cells transformed by the prolonged, constitutive expression of the viral oncogene.

Inhibition of HO-1 by SnPP and shRNA Impairs vGPCR-transforming Activity in Cultured NIH3T3 Fibroblasts—Considering that vGPCR induced the expression of HO-1 and that higher enzyme levels result in higher enzymatic activity (2), we next explored whether inhibiting both the activity and transcription of HO-1 impaired vGPCR-transforming capability. Accordingly, we performed focus formation assays transfecting NIH3T3 cells with 1 mg/plate of pCEFL-vGPCR and cultured them for a period of 3–4 weeks with or without adding the HO-1 inhibitor SnPP to the 5% calf serum-containing culture media. SnPP, a metalloporphyrin formed by a chelate of tin with the porphyrin ring, has proven to be one of the most efficient inhibitors of HO-1 both *in vitro* and *in vivo* (26–29) and regulates heme oxygenase by a dual mechanism. It enhances the synthesis of new protein but potently inhibits the enzyme at the catalytic site by acting as a competitive substrate for heme. Inhibition of heme oxygenase by SnPP is so pronounced that, despite the marked increase in the synthesis of new enzyme, suppression of heme oxidation is the prevailing biological effect (30). As seen in Fig. 3*A*, addition of 50–100 μM of SnPP twice a week, strongly reduced the appearance of foci when compared with control plates. This effect was so marked that led us to investigate whether SnPP affected specifically vGPCR-induced foci or had an effect on transformation induced by other oncogenes. For example, although a direct correlation between a classical oncogene like Ras and HO-1 has not been reported, pancreatic cancers have a high incidence of Ras mutations (31) and HO-1 overexpression (32). Thus, we transfected NIH3T3 cells with an activated form of Ras (Ras V12) and scored foci formation after 2 weeks. Interestingly, the appearance of Ras V12-induced foci was also reduced by SnPP, suggesting that HO-1 could be a common target and mediator of transforming oncogenes.

Despite the fact that the HO-2 isoform was not induced by vGPCR and was expressed at very low levels in NIH3T3 and vGPCR-transformed cells (see Fig. 2*E*), we could not discard that the inhibitory effect of SnPP was due to a general inhibition of the two HO isoforms. Thus, we studied whether targeted knock-down of HO-1 expression had a similar result on vGPCR transforming activity. Knock-down of HO-1 mRNA was achieved by transfection of a shRNA targeted to a mouse HO-1 region highly conserved in human HO-1 previously shown to be an effective target for RNA interference (33). To corroborate the capability of the shRNA HO-1 to reduce vGPCR-induced HO-1 levels in our model, we transfected NIH-vGPCR cells with 10 μg of the shRNA for HO-1 cloned in the pSilencer vector (pS-shRNAHO-1) or pSilencer alone (pS-shRNA) used as a control, along with 100 ng of the pCEP4 plasmid to allow for the antibiotic selection of transfected cells. After selection, the two new cell lines, NIH-vGPCR$_{shRNAHO\text{-}1}$ (carrying the shRNA for HO-1) and NIH-vGPCR$_{shRNA}$ (control), were assayed for endogenous HO-1 expression levels. As shown in Fig. 3*B*, protein extracts from NIH-vGPCR$_{shRNAHO\text{-}1}$ displayed a 68% reduction in HO-1 levels with respect to NIH-vGPCR$_{shRNA}$. To confirm that the shRNA for HO-1 specifically knocked down only the enzyme, we analyzed the levels of HO-2, vGPCR, and the housekeeping gene GAPDH. As expected, the HO-2 levels detected were not different between the two cell lines, and similarly, the shRNA for HO-1 did not affect the expression of vGPCR or GAPDH (Fig. 3*B*). Based on these evidences, we carried out focus formation assays culturing 5×10^4 NIH-vGPCR$_{shRNA}$ or NIH-vGPCR$_{shRNAHO\text{-}1}$ on a 50% confluent monolayer of NIH3T3 cells. As shown in Fig. 3*C*, targeted knock-down of HO-1 expression strongly reduced the transforming capability of vGPCR-expressing cells. Taken together, these results indicate that HO-1 expression and activity played and important role in mediating the oncogenic activity of vGPCR in NIH3T3 fibroblasts.

starvation, they were harvested, stained with annexin V-PE and 7-AAD, and sorted by flow cytometry. Viable cells are shown in the *lower left quadrant*, whereas cells in early apoptosis and positive for annexin V-PE are shown in the *lower right quadrant*. Results shown are representative of triplicate experiments. *D*, cells were transfected with 10 ng of pHO1-Luc and 100 ng of p*Renilla*-Luc and serum-starved for 24 h. Lysates were assayed for *Firefly* and *Renilla* luciferase activities. The data represent average *Firefly* luciferase activity normalized by *Renilla* luciferase activity in each sample ± S.E. from triplicates expressed as fold induction for NIH-vGPCR cells relative to values in NIH3T3 cells. Similar results were obtained in three additional experiments. *E*, NIH3T3 and NIHvGPCR cells were serum-starved for 24 h. NIH3T3 cells were untreated or exposed to 10 μM hemin for 4 h as indicated, and total RNA was isolated. HO-1 and GAPDH levels were detected by RT-PCR. Products were visualized by ethidium bromide staining after electrophoresis (*upper panels*). Parallel samples were analyzed for HO-1 and HO-2 by Western blot with specific monoclonal antibodies for each protein (*lower panels*).

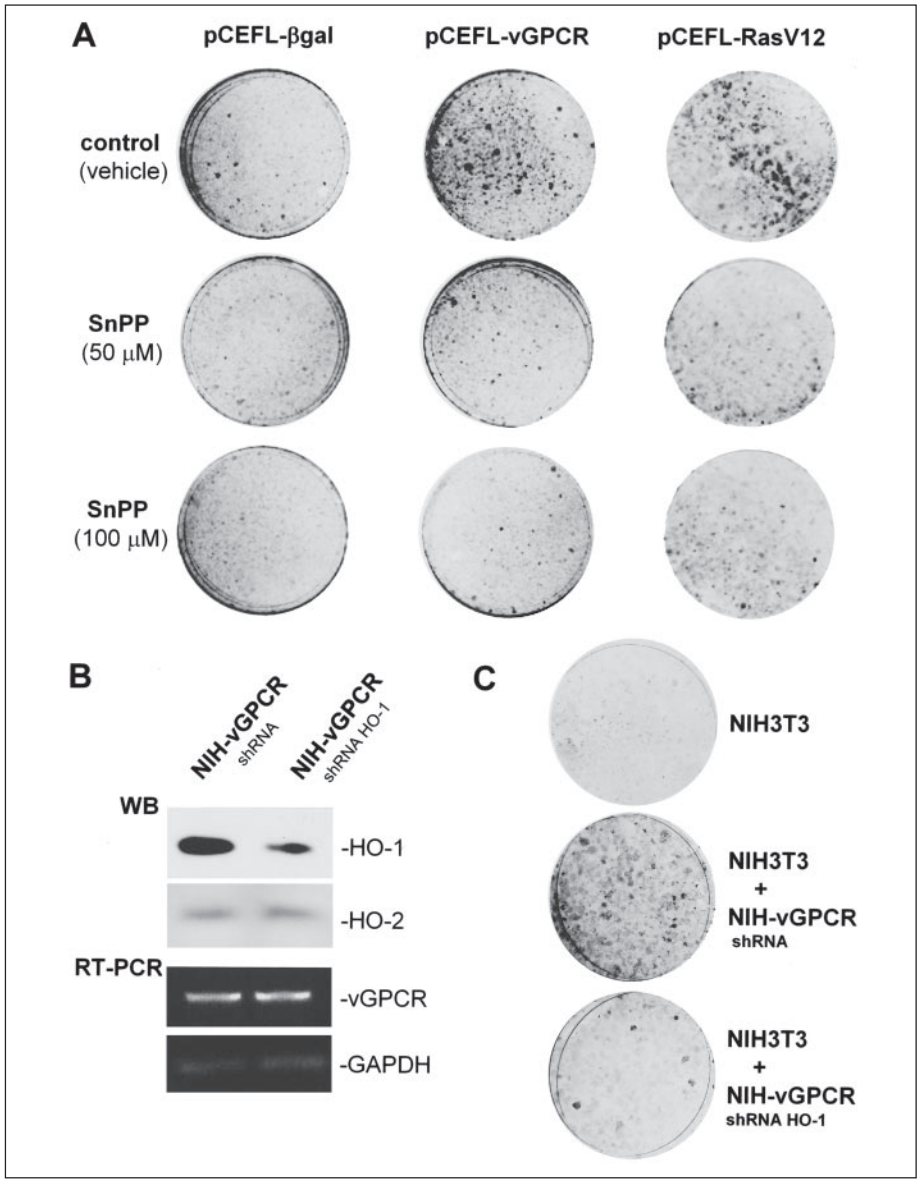

FIGURE 3. **Inhibition of HO-1 expression and activity impairs vGPCR-transforming activity.** *A*, NIH3T3 cells were transfected by the calcium phosphate technique with 1 μg of pcDNAIII-β-gal, 1 μg of pCEFL-vGPCR, or 100 ng of pCEFL-AU5-Ras V12, as indicated. Cells were cultured in 5% calf serum with or without addition of 50–100 μM SnPP. After 3 weeks, plates were fixed and stained to score foci formation. The plates shown are representative of three different experiments. *B*, NIH-vGPCR stably transfected with pS-shRNA (NIH-vGPCR$_{shRNA}$) or pS-shRNAHO-1 (NIH-vGPCR$_{shRNAHO-1}$) were starved for 24 h. Cells were lysed, and protein extracts were assayed for HO-1 and HO-2 by Western blot using specific mouse monoclonal antibodies (*upper panels*). Total RNA was isolated from parallel plates, and vGPCR levels were detected by RT-PCR (*lower panel*). *C*, 5×10^4 NIH-vGPCR$_{shRNA}$ and NIH-vGPCR$_{shRNAHO-1}$ cells were cultured on a monolayer of NIH3T3 cells, as indicated. After 3 weeks, plates were fixed and stained to score foci formation. Representative plates from three different experiments are shown.

HO-1 Mediates vGPCR-induced Survival and Proliferation in Endothelial Cells—Several studies show that the characteristic spindle cells of the KS lesion that provoke the angiogenic process typical of this neoplasia are derived from the KSHV infection of endothelial cells (13, 34). Moreover, recent evidence demonstrates that the sole infection of endothelial cells with vGPCR causes endothelial cell immortalization (35) and KS-like lesions in an animal model (18). On the other hand, a direct effect of HO-1 as a regulator of endothelial cell growth (36, 37) and apoptosis (38) has been shown, and several studies highlight the central role of the enzyme in the regulation of angiogenesis (3). Based on this, we compared the effect of vGPCR or HO-1 overexpression on endothelial cell growth. We first engineered an expression vector carrying an HA tagged-form of a full-length cDNA for mouse HO-1 (pCEFL-HA-HO-1). Immunofluorescence assays using a specific anti-HA antibody showed that transiently transfected HA-HO-1 localized to microsomal membranes. Only HA-HO-1-transfected cells were stained positively with the anti HA antibody (Fig. 4*A*). Its cell localization was similar to that of the endogenous enzyme, detected by a specific anti-HO-1 antibody, when induced by AU5-vGPCR (data not shown). Next, we stably transfected endothelial cells with pCEFL (SVEC), pCEFL-vGPCR (SVEC-vGPCR), and pCEFL-HA-HO-1 (SVEC-HA-HO-1). After several passages in culture, all three cell lines were serum-starved for 48 h and analyzed for vGPCR, HO-1, and GAPDH mRNA expression levels by semiquantitative RT-PCR. As shown in Fig. 4*B*, HO-1 mRNA levels in SVEC were very low, whereas constitutive expression of vGPCR induced HO-1 mRNA by 3.3-fold with respect to SVEC. As expected, the mRNA for the enzyme was increased in SVEC-HA-HO-1 cells (4.65-fold). These changes were confirmed by Western blot assays where again the levels of the enzyme were low in SVEC and were increased in SVEC-vGPCR cells. The expression levels of HA-HO-1 and endogenous HO-1 in SVEC-HA-HO-1 are displayed in Fig. 4*C* (*last lane*). Of note, the level of endogenous HO-1 was also induced in comparison with SVEC, most likely through a positive regulation loop in which HO-1-generated heme by-products initiate signaling cascades that act on the *ho-1* promoter (3) (Fig. 4*C*).

SVEC-vGPCR and SVEC-HA-HO-1 cells displayed faster growth rates than SVEC (data not shown). As cell growth results from the balance between cell death and proliferation, we performed experiments to determine the effect of constitutive HO-1 expression on endothelial cell apoptosis and proliferation. First, we explored apoptotic

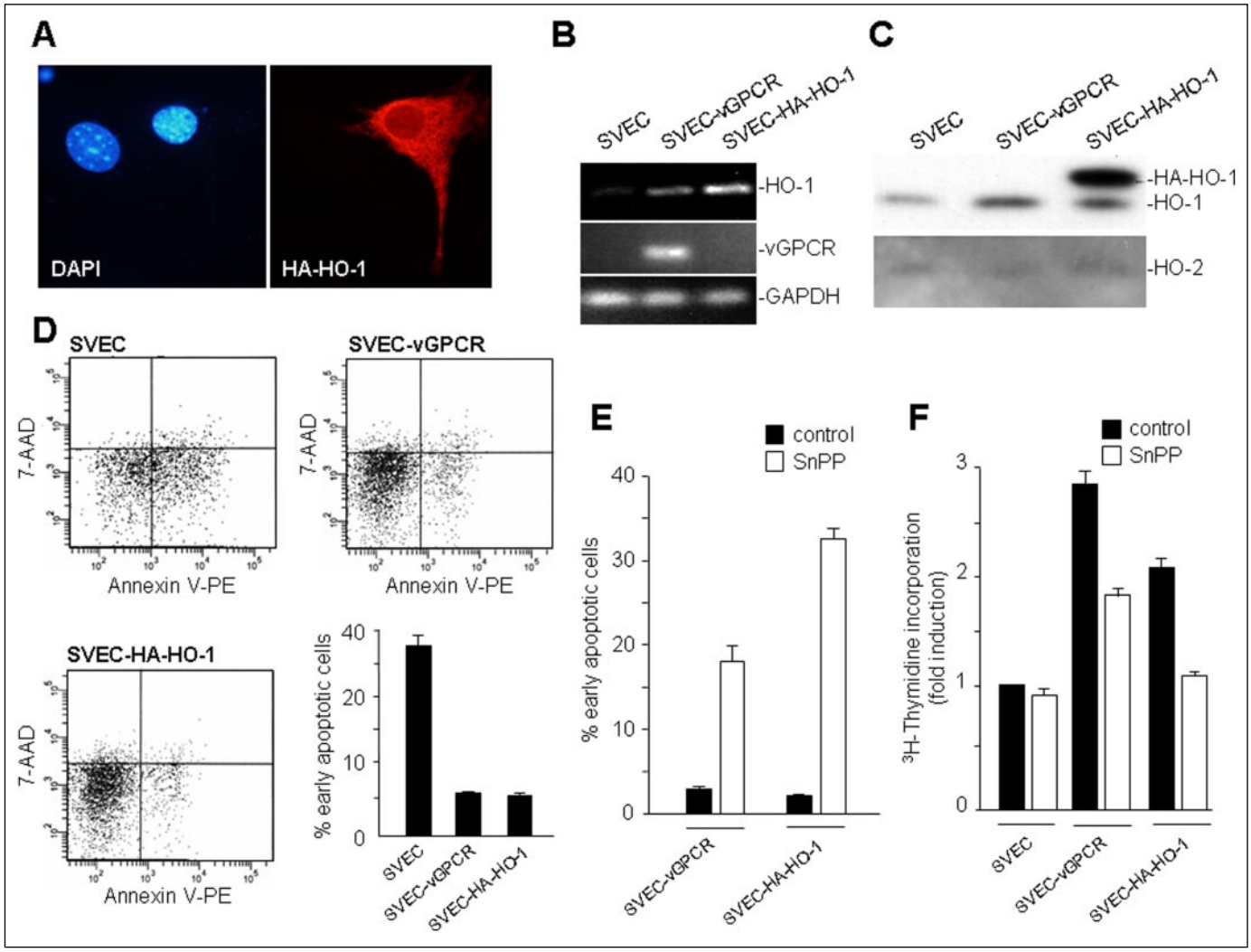

FIGURE 4. **HO-1 as a mediator of vGPCR-induced survival and proliferation.** *A*, cells were seeded in coverslips and transfected with pCEFL-HA-HO-1. After 24-h serum starvation, cells were fixed and analyzed by immunofluorescence with DAPI nuclear staining and for HA-HO-1 with an anti HA monoclonal antibody. *B*, SVEC, SVEC-vGPCR, and SVEC-HA-HO-1 cells were serum-starved for 24 h, and total RNA was isolated. HO-1, vGPCR, and GAPDH levels were detected by RT-PCR. Products were visualized by ethidium bromide staining. *C*, cells were cultured as above and protein extracts were analyzed for HO-1 and HO-2 expression by Western blot with specific monoclonal antibodies for each protein. *D*, cells were cultured as above and after 48-h serum starvation, harvested, stained with annexin V-PE and 7-AAD, and sorted by flow cytometry. Viable cells are shown in the *lower left quadrant*, whereas cells in early apoptosis and positive for annexin V-PE are shown in *lower right quadrant*. The percentage of early apoptotic cells is shown in the *lower left graphic*. Results shown are representative of triplicate experiments. *E*, SVEC-vGPCR and SVEC-HA-HO-1 cells were treated with vehicle (*control*) or 100 μM SnPP. After 48-h treatment under serum starvation, early apoptosis was detected as above. Depicted percentages of apoptotic cells are the average ± S.E. of triplicate experiments. *F*, cells were serum-starved and treated with vehicle (*control*) or 100 μM SnPP for 48 h and exposed to [^{3}H]thymidine for 2 h. Results are the average of incorporated radioactivity among triplicate samples normalized by total protein ± S.E. and expressed as fold induction relative to SVEC. Similar results were obtained in three independent experiments.

changes by annexin V-PE and 7-AAD staining. As expected, 48 h after serum starvation, SVEC-vGPCR showed reduced levels of annexin V-PE staining (6%) when compared with SVEC (37%). Notoriously, SVEC-HA-HO-1 behaved similarly to SVEC-vGPCR as their levels of apoptosis where nearly identical (5.7%) (Fig. 4*D*, *lower right quadrants* and *bottom right panel*). These data suggest that HO-1 *per se* induced endothelial cell survival in a manner comparable with that of vGPCR.

Taking the above results into account, we set out to determine whether inhibiting HO-1 with SnPP would block vGPCR-induced survival. In an independent experiment, we observed that 48-h treatment with 100 μM tin protoporphyrin increased the percentage of apoptotic cells from 4.5 to 17.5% in SVEC-vGPCR and from 3.5 to 33.2% in SVEC-HA-HO-1 (Fig. 4*E*). Interestingly, the effect of SnPP was more pronounced in SVEC-HA-HO-1 than in SVEC-vGPCR cells; as upon treatment, the levels of apoptosis in the first cell line were comparable with those of normal SVEC cells (33.2 and 36%, respectively) (Fig. 4, *D* and *E*, and data not shown). Similarly, in cells growing in 10% serum-supplemented media, only 5.7% was annexin V-PE-positive after SnPP treatment, indicating that both vGPCR and serum activated alternative, HO-1-independent mechanisms of survival. Similar results were obtained in parallel experiments performed in NIH3T3, NIH-vGPCR, and NIH-HO-1 cells (data not shown). Together, these data suggest that increased expression of HO-1 had a protective effect on cell viability and that the enzyme played an important role in vGPCR-induced fibroblast and endothelial cell survival.

To assess the effect of HO-1 overexpression in cell proliferation, we performed [^{3}H]thymidine incorporation assays in all three SVEC cell types after a 48-h serum starvation period. As shown in Fig. 4*F*, thymidine incorporation was increased by 3- and 2-fold in SVEC-vGPCR and SVEC-HA-HO-1 cells, respectively, with respect to SVEC and after normalization by total amount of proteins. Noteworthy, this uptake was practically abolished by preincubating the cells for 48 h with 100 μM SnPP in SVEC-HA-HO-1 cells and reduced in a 52% in SVEC-vGPCR. On the contrary, the tin protoporphyrin did not affect significantly the

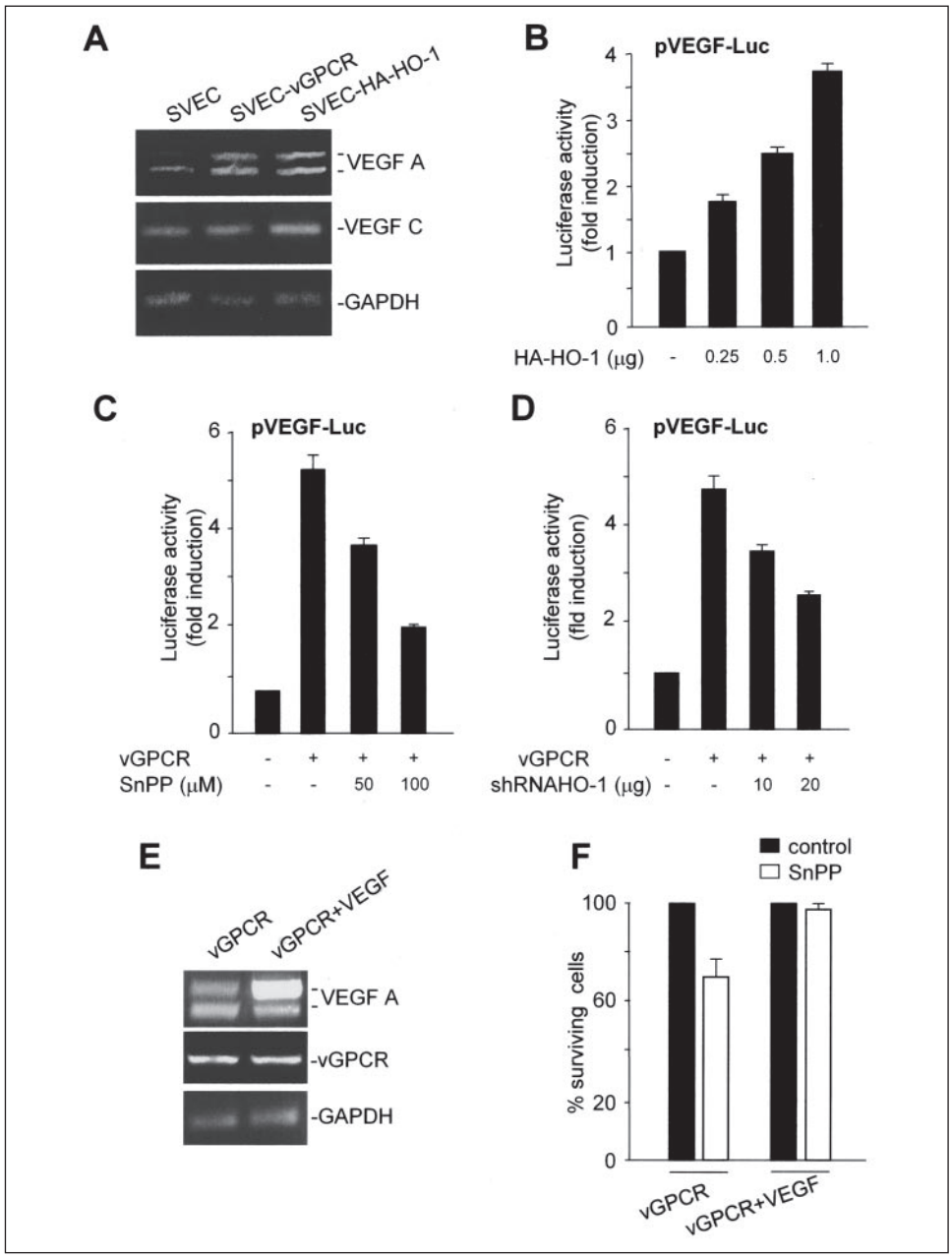

FIGURE 5. **HO-1 mediates vGPCR-induced VEGF expression.** *A*, SVEC, SVEC-vGPCR, and SVEC-HA-HO-1 cells were serum-starved for 24 h, and total RNA was isolated. VEGF-A, VEGF-C, and GAPDH mRNA levels were detected by RT-PCR. Products were visualized by ethidium bromide staining after electrophoresis in a 2% agarose gel. *B–D*, cells were cotransfected with 25 ng of pVEGF-Luc, different amounts of pCEFL-HA-HO-1, 1 μg of pCEFL-vGPCR, and different amounts of pS-shRNAHO-1 along with 100 ng of p*Renilla*-Luc as indicated. The total amount of plasmid DNA in each transfection was equally adjusted with pcDNA3-β-galactosidase. 3 h after transfection, cells were serum-starved and incubated with vehicle or 50–100 μM SnPP as shown. 24 h later, lysates were assayed for *Firefly* and *Renilla* luciferase activities. The data represent average *Firefly* luciferase activity normalized by *Renilla* luciferase activity in each sample ± S.E. from triplicates. Similar results were obtained in three additional experiments. *E* and *F*, vGPCR+VEGF-expressing cells were cultured and serum-starved for 48 h. VEGF-A, vGPCR, and GAPDH levels were determined by RT-PCR from total RNA isolated from the indicated cells. Under the same conditions, parallel cells were assayed for apoptosis by annexin V-PE staining. Results are means from three different experiments, and values are depicted as percentage of SnPP-treated surviving cells relative to control surviving cells for each cell line taken as 100%.

basal level of [^{3}H]thymidine incorporation of serum-starved SVEC and only slightly decreased it in serum-induced SVEC (Fig. 4*F* and data not shown). All in all, these results support the hypothesis of a major role for HO-1 in the control of vGPCR-regulated endothelial cell growth both at the survival and proliferative levels.

HO-1 Mediates vGPCR-induced VEGF Expression—Several findings suggest that vGPCR participates in KS pathogenesis by driving spindle cell formation, growth, and angiogenesis in a paracrine fashion, by inducing the expression and secretion of VEGF (17, 35), an angiogenic growth factor central in the process of new blood vessel formation in tumors (39). Considering that NIH3T3 cells stably expressing vGPCR secrete high levels of VEGF A (16, 40), we investigated whether SVEC-vGPCR and SVEC-HA-HO-1 had a comparable, increased expression of this growth factor by RT-PCR using primers that amplify three murine splice variants of VEGF-A (VEGF120, -164, and -188) (20). Under the number of cycles used to keep the amplification in the linear phase (28 cycles) only VEGF120 and VEGF164 were detected (431- and 563-bp bands, respectively). As shown in Fig. 5*A*, both cell lines exhibited approximately a 3-fold induction in total VEGF mRNA levels when compared with SVEC. Because some studies indicate that vGPCR has an effect on the expression of the VEGF-C (19, 41), we tested whether the viral oncogene or HO-1 were able to induce its expression. Fig. 5*A*, *middle panel*, shows that the levels of VEGF-C were only slightly up-regulated in HO-1 expressing cells whereas no changes were observed in SVEC-vGPCR when compared with SVEC. Based on this, we evaluated the effect of transient transfection of different amounts of HO-1 on a *vegf-a* promoter-driven reporter luciferase gene (pVEGF-Luc) and found that the promoter responded to HO-1 overexpression in a dose-dependent manner, which corroborated that HO-1 was able to affect VEGF-A expression (Fig. 5*B*).

To investigate whether HO-1 mediated vGPCR-induced VEGF expression, we transfected cells with pCEFL-vGPCR and pVEGF-Luc. Fig. 5*C* shows that a 24-h treatment with 50 and 100 μM SnPP strongly reduced vGPCR-induced pVEGF-Luc activity, indicating that HO-1

mediates the effect of the viral oncogene on the activity of the *vegf* promoter. To corroborate the effect of HO-1, we repeated the experiment cotransfecting cells with pS-shRNAHO-1. As depicted in Fig. 5*D*, increasing amounts of shRNAHO-1 impaired considerably the stimulatory effect of vGPCR on pVEGF-Luc activity. Thus, HO-1 might parallel the effect of vGPCR on endothelial cell growth by stimulating VEGF expression. To confirm this hypothesis, we stably transfected vGPCR-expressing cells with a plasmid carrying a full-length cDNA for VEGF165, the human homologue of mouse VEGF164. To corroborate VEGF165 expression after antibiotic cell selection, we performed semiquantitative RT-PCRs using the primers described above as they amplify highly homologous regions in mVEGF164 and hVEGF165. Thus, cells stably transfected with vGPCR + hVEGF165 showed stronger amplification of the upper 563-bp band, indicating hVEGF165 isoform overexpression. Equal vGPCR expression was verified, and amplification of GAPDH was used as a control (Fig. 5*E*). Interestingly, 48-h treatment with the HO-1 inhibitor SnPP under serum starvation conditions did not affect vGPCR + VEGF expression cell survival in contrast to the effect of SnPP on vGPCR-expressing cells (Fig. 5*F*). These data show that the constitutive expression of VEGF rescued the inhibitory effect of SnPP on vGPCR-induced cell survival and strongly suggest that VEGF-A might be a downstream component in the vGPCR/HO-1/survival pathway (Fig. 5*F*).

We next asked whether HO-1 activity impairment solely reduced vGPCR-induced VEGF expression or if this enzyme also mediated hypoxia- and cytokine-induced VEGF expression (42, 43). As shown in Fig. 6*A*, $CoCl_2$, a well known inductor of hypoxia, induced both HO-1 and VEGF expression as judged by the results of semiquantitative RT-PCRs. Interestingly, this effect was not blocked by SnPP, indicating that hypoxia induces VEGF through an HO-1-independent mechanism, as reported recently (44). However, when VEGF expression was induced by the cytokine IL-6 (100 ng/ml), SnPP blocked this induction by a 63% indicating that HO-1 was at least partially required for cytokine-induced VEGF expression. Interestingly, the CoPP (10 mM), an inducer of HO-1 expression, also induced VEGF, but its effect was almost entirely blocked by preincubation with SnPP. These results are in line with recent findings showing that CoPP requires HO-1 activity to induce VEGF expression (44) and that overexpression of HO-1 is sufficient to trigger VEGF expression (45). Of note and as expected, SnPP did not block $CoCl_2$, IL-6, or CoPP-induced HO-1 expression but on the contrary increased it. This showed directly the dual effect of SnPP both as an inducer of HO-1 expression and indirectly as an inhibitor of its enzymatic activity. None of these treatments altered the expression of GADPH used as a control. Altogether, these data suggest that the requirement for HO-1 in vGPCR-induced VEGF expression might be common to several angiogenic factors and effectors.

Inhibition of HO-1 Enzymatic Activity by SnPP Impairs vGPCR-induced Tumorigenesis in Mice—Whereas parental NIH3T3 and SVEC cells are non-transformed, they acquire the capability to form foci in cell culture models and to induce tumors in nude mice when transformed by an oncogene. Thus, vGPCR-overexpressing NIH3T3 and SVEC cells, but not the parental cells, have been reported to induce tumors when injected into nude mice (16, 24). Prompted by our findings, we used these models to investigate whether inhibiting HO-1 could affect vGPCR-induced tumorigenesis *in vivo*. We first injected 1×10^6 SVEC-vGPCR cells into the right flank of nude mice, and 20 days after cell injection, all mice developed one tumor of ~3–4 mm in diameter. At this point, mice were split in three groups of five animals each and subjected to a daily subcutaneous administration near the tumor area of vehicle (control), a 10 μmol/kg dose of SnPP, or a 10 μmol/kg dose of

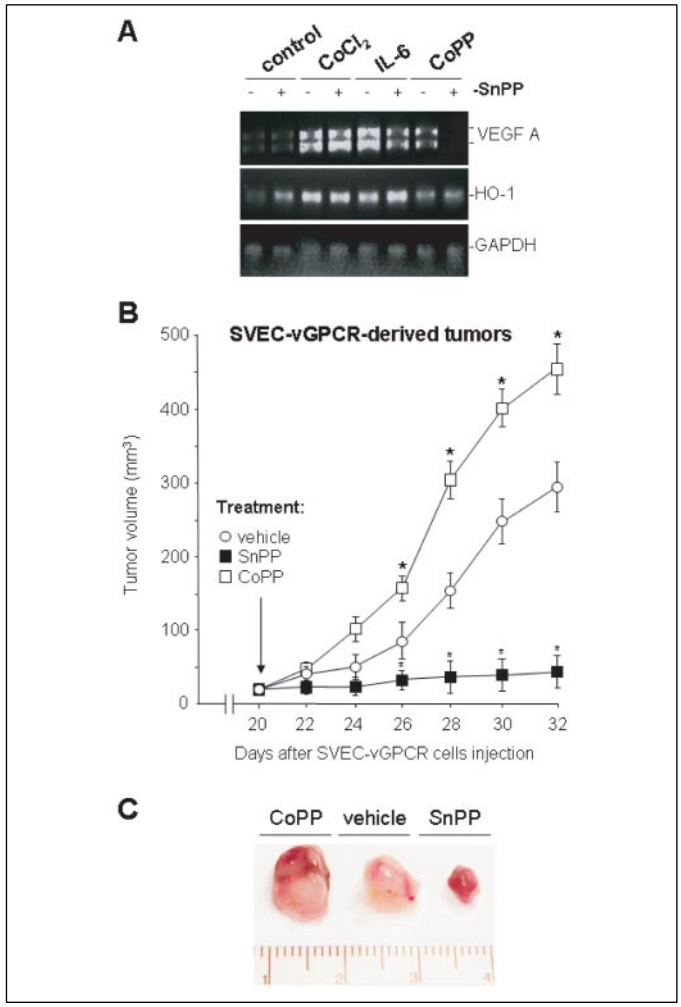

FIGURE 6. **SnPP and CoPP have opposite effects on VEGF expression and vGPCR-induced tumor growth.** *A*, SVEC cells were serum-starved for 24 h and pretreated with or without 50 μM SnPP followed by a 6-h treatment with vehicle, 100 ng/ml IL-6, 250 μM $CoCl_2$, or 10 μM CoPP. After treatment, total RNA was isolated and VEGF-A, HO-1, and GAPDH mRNA levels were detected by RT-PCR. Products were visualized by ethidium bromide staining. *B*, 1×10^6 SVEC-vGPCR cells were injected in the right flank of 15 nude mice. 20 days after cell injection, animals were split in three groups (five mice each) and treated with vehicle (0.1 N NaOH in PBS, pH 7.4), 10 μmol/kg of body weight of SnPP or CoPP, injected subcutaneously on a daily basis. Tumor volumes were measured every other day. Data are mean ± S.E. (*, $p < 0.05$ for SnPP- and CoPP-treated animals compared with vehicle in the same day measurement). *C*, representative tumors from vehicle-, SnPP-, or CoPP-treated animal removed after 12-day treatments.

CoPP. Tumor growth in each mouse was scored every other day. After 12-day treatments, tumor growth was significantly suppressed in mice receiving SnPP, as the average tumor volume was reduced by nearly 84% ($V = 0.044 \pm 0.007$) with respect to control animals ($V = 0.289 \pm 0.074$ cm^3). Contrarily, CoPP-treated animals presented larger tumors than controls ($V = 0.464 \pm 0.068$) (Fig. 6*B*). CoPP- and SnPP-treated tumors were darker than control tumors most likely due to the accumulation of the red-colored protoporphyrin solutions (Fig. 6*C*). These remarkable opposite effects of SnPP and CoPP on vGPCR-induced tumor growth provide evidence for the importance of HO-1 activity in the oncogenic cell growth process.

To discern whether the effect of SnPP was due to inhibition of vGPCR-induced HO-1 within the tumor or to a general reduction of the HO-1 activity in the animal that somehow affected tumor growth, we injected 1×10^6 NIH-vGPCR$_{shRNA}$ and NIH-vGPCR$_{shRNAHO-1}$ cells in the right side flank of nude mice (five mice per group). As shown in Fig. 3*B*, these two cell lines present identical levels of vGPCR, HO-2, and

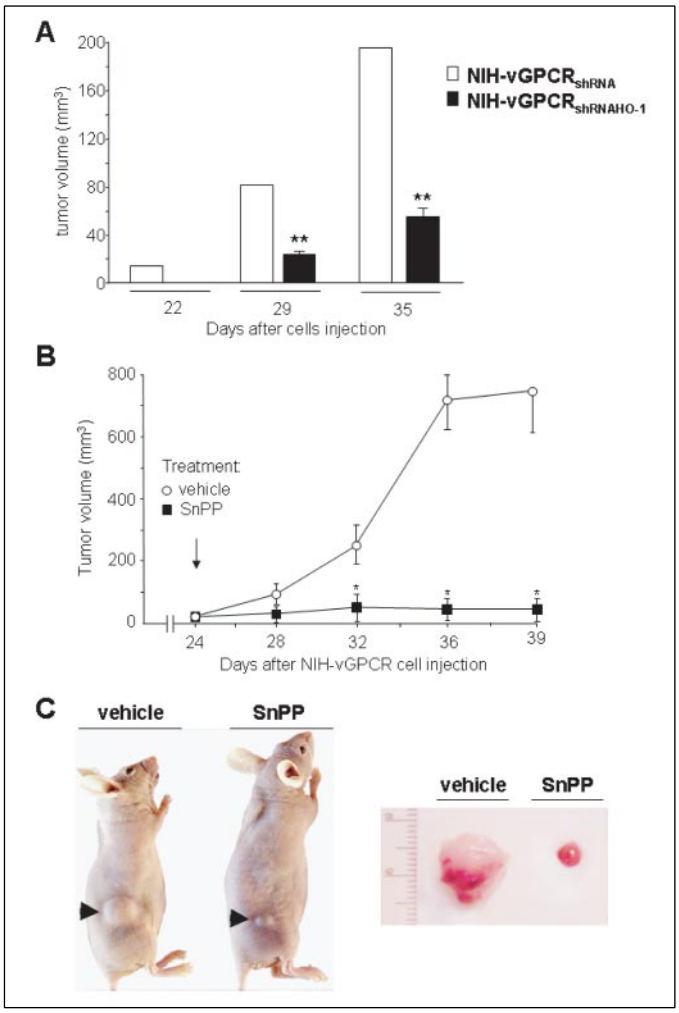

FIGURE 7. **HO-1 expression and activity are required for vGPCR-induced tumorigenesis in mice.** *A*, 1×10^6 NIH-vGPCR$_{shRNA}$ or NIH-vGPCR$_{shRNAHO-1}$ cells were injected subcutaneously in the right flank of five nude mice. 22, 29, and 35 days after injection, tumor volumes were measured. Data are mean ± S.E. from $n = 5$ in each group, expressed as tumor volume (**, $p < 0.01$). *B*, 1×10^6 NIH-vGPCR cells were injected as above in 10 nude mice. 24 days after injection, animals were split in two groups and administered subcutaneously twice a week with 10 μmol/kg of body weight SnPP or vehicle. Tumor volumes were measured every 3 days. Data are mean ± S.E. from $n = 5$ (*, $p < 0.05$ for SnPP-treated animals compared with controls in the same-day measurement). *C*, tumor-bearing animals and surgically removed tumor from a representative mouse from each group after 15 days of SnPP or vehicle administration are depicted.

GADPH, but the level of HO-1 has been reduced in 68% in NIH-vGPCR$_{shRNAHO-1}$ cells with respect to NIH-vGPCR$_{shRNA}$ by means of a specific shRNA for HO-1. Tumors started to be noticeable around 20 days after cell injection in mice injected with NIH-vGPCR$_{shRNA}$ (2–3 mm in diameter) and around 23–26 days in animals injected with NIH-vGPCR$_{shRNAHO-1}$. In addition to this initial delay in tumor development, measurement of tumor size 1 week later revealed a nearly 61% reduction in tumor volume in those generated by NIH-vGPCR$_{shRNAHO-1}$ cells ($V = 0.0275 \pm 0.014$), when compared with those from NIH-vGPCR$_{shRNA}$ cells ($V = 0.0719 \pm 0.017$). Two weeks later the difference was more pronounced reaching a 72% ($V = 0.0538 \pm 0.019$ cm^3 *versus* $V = 0.193 \pm 0.02$ cm^3) (Fig. 7*A*). The remarkable parallelism between tumor growth and HO-1 expression reductions pointed out HO-1 as a major mediator in the process of vGPCR-induced tumor growth.

To discard cell type-specific effects, we next analyzed the result of systemic SnPP administration to animals bearing tumors derived from NIH-vGPCR cells. Each mouse developed one tumor measurable 24 days after cell injection. At that point, animals were separated in two different groups and received vehicle or 10 μmol/kg SnPP twice a week. Tumor growth reduction after 15 days of SnPP administration was remarkable, as average tumor size was reduced by nearly 94% in SnPP-treated animals ($V = 0.0378 \pm 0.008$) ($n = 5$) when compared with control mice ($V = 0.742 \pm 0.145$) ($n = 5$) (data not shown) (Fig. 7*B*). A representative tumor-bearing animal and a tumor representative from each group after 15-day treatments are depicted in Fig. 7*C*. Interestingly, the SnPP-treated group had a darker, reddish skin tone (Fig. 7*C*), most likely due to the accumulation of the inhibitor in this organ (46). Except for this and a slight darker color in liver and spleen, no other internal organ macroscopic change either in morphology or size was observed in SnPP-treated animals with respect to controls (data not shown). Similarly, vehicle- and SnPP-treated animals showed no differences in body weight and general behavior, which indicates the lack of apparent toxic secondary effects of the SnPP during the length of the experiment. Moreover, histological examination of liver and skin sections showed the absence of tissue necrosis in both groups (data not shown). Overall, the striking consequence of impairing HO-1 expression and/or activity on vGPCR-driven tumor growth pointed out the major role of the enzyme in the process of unregulated, aberrant cell growth *in vivo*.

SnPP Inhibits HO-1 Activity and Reduces VEGF Expression in vGPCR-induced Tumors—As HO-1 expression has been detected in biopsy tissue of oral AIDS-KS lesions, we investigated whether HO-1 expression was also up-regulated in vGPCR-driven tumors. Thus, we assessed protein levels by immunohistochemistry in tumor, liver, and skin histological sections from the same animals using a specific anti HO-1 antibody. As seen in Fig. 8*A* (*left* and *middle panels*), tumors showed higher HO-1 reactivity than liver, used as a staining positive control (28). In contrast, HO-1 was almost undetectable in skin tissue removed from the area above the tumor, confirming the specificity of the immunodetection (Fig. 8*A*, *right panel*). Hematoxylin staining of all tissue sections is shown in Fig. 8*A*, *lower panels*.

Next, to confirm that tumor growth suppression in SnPP-treated animals (Fig. 7*B*) was a consequence of the delivery of subcutaneously injected SnPP to tumor cells and to the inhibition of HO-1 activity, we set up *in vitro* HO-1 activity assays with microsomal protein samples from three control and three SnPP-treated tumors. As shown in Fig. 8*B*, measurable HO-1 activity was detected in microsomal samples from control tumors as evidenced by the *in vitro* synthesis of bilirubin. This activity was higher than that from liver microsomes, used as a control (data not shown). As expected, HO-1 activity was nearly abolished in samples obtained from SnPP-treated tumors, which validated the use of SnPP as a potent *in vivo* inhibitor of the enzyme. To confirm the above findings, we carried out Western blot analysis of the microsomal fractions and found that indeed control tumors expressed high levels of HO-1 (Fig. 8B, *lower panel*). HO-1 expression was increased in SnPP-treated tumors by 2.6-fold when compared with controls, as this protoporphyrin is able to simultaneously induce HO-1 expression while inhibiting the enzyme, as mentioned above (30). Identical results were obtained by immunohistochemical detection of HO-1 when comparing tumor sections from control and SnPP-treated animals (data not shown). Of note, HO-1 from SnPP-treated samples showed a slight gel retardation, most likely due to binding of the protoporphyrin to the HO-1 heme binding domain (30, 47). No differences were observed in the amounts or mobility of the control microsomal PDI in microsomes samples from control or SnPP-treated tumors. These data confirmed that subcutaneous administration of SnPP allowed the drug to reach tumor cells and to strongly inhibit HO-1 activity.

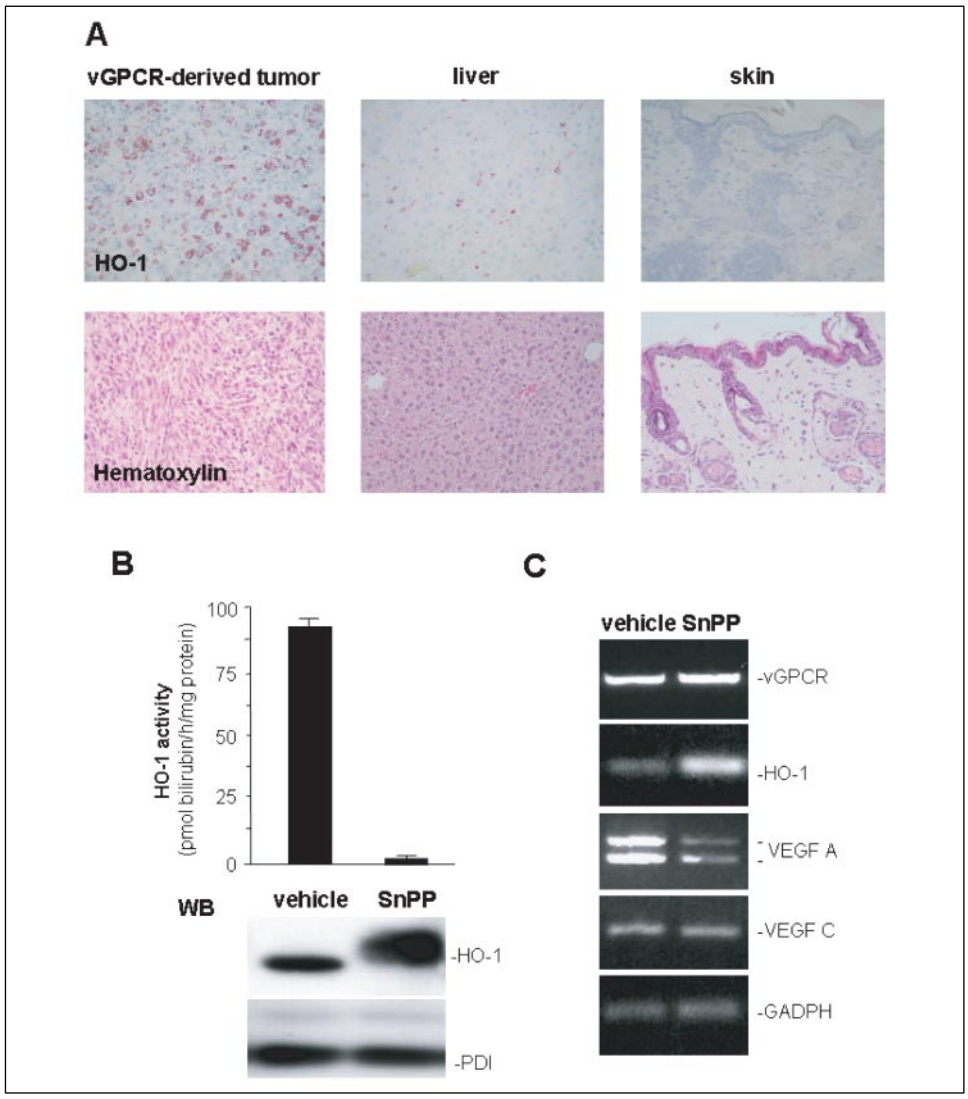

FIGURE 8. **HO-1 is expressed in vGPCR-induced tumors, and its activity is inhibited by SnPP treatment.** *A*, tumor, liver, and skin tissue sections from control mice were stained with an antibody against heme oxygenase-1 (*upper panels*) and with hematoxylin (*lower panels*). *B*, 24 h after vehicle and SnPP injection in mice treated for 15 days, tumors and livers from three animals from each group were obtained. After microsomal fraction purification, *in vitro* HO activity (*upper panel*) was assayed. Results are expressed as picomoles of bilirubin formed per milligram of microsomal fraction per hour and are the mean ± S.E. from triplicates. Western blot detection of HO-1 and PDI was performed on aliquots from the same microsomes (*lower panels*). *C*, expression of vGPCR, HO-1, VEGF-A, VEGF-C, and GAPDH mRNA in the above tumors was detected by RT-PCR followed by ethidium bromide staining of the PCR products. Bands shown are representative of three tumors analyzed per group of control and SnPP-treated mice.

To discard the possibility that the impaired tumor growth was due to changes in vGPCR expression, we carried out semiquantitative RT-PCR assays. Using identical amounts of total-RNA initial template, we observed that indeed, both control and SnPP-treated tumors expressed similar amounts of vGPCR, thus discarding an inhibitory effect of SnPP on the levels of the oncogene (Fig. 8*C*, *first panel*). We also observed that HO-1 mRNA expression was clearly detected in control tumors samples and further increased in SnPP-treated tumors, in agreement with the above Western blot results. However, despite the stimulatory effect of SnPP on HO-1 expression, the levels of VEGF-A mRNA were reduced by 75% when compared with control tumors. This confirmed the effect of SnPP on vGPCR-induced VEGF-A expression *in vivo* and paralleled the results found in the cell culture models. Instead, the levels of VEGF-C were not significantly affected by SnPP. Amplification of GAPDH mRNA was used as a control. Nearly identical results were obtained by analyzing mRNA samples from tumors developed from SVEC-vGPCR cells, which indicates that HO-1 mediates vGCPR-dependent tumor growth most likely by a common mechanism that involves the regulation of VEGF-A expression in the two experimental models.

Considering the uniform tendency of the results, the data postulate HO-1 as important mediator of vGPCR-induced tumor growth and suggest that inhibition of intratumoral HO-1 activity by SnPP may be a potential therapeutic strategy.

DISCUSSION

Recent findings showing elevated expression levels of HO-1 in biopsies from tumors of KS patients (12) prompted us to investigate whether vGPCR, one of the key genes involved in the development of KS, was able to induce the constitutive expression of HO-1. In this study we show that indeed, vGPCR up-regulated the expression of HO-1 in murine fibroblasts and endothelial cells. Moreover, histological sections of solid mouse tumors derived from injection of vGPCR-expressing cells displayed significant levels of HO-1. Our data suggest that HO-1 plays an important role in vGPCR-induced cellular survival, proliferation, and transformation, as targeting HO-1 enzymatic activity with the tin protoporphyrin IX (SnPP) and its expression with shRNA significantly reduced the effects of the viral oncogene both in cellular and animal tumor models.

To the best of our knowledge, this is the first study showing that a viral oncogene promotes HO-1 gene expression. The signal transduction pathways involved are not known. By using small molecule inhibitors and dominat negative mutants, we have observed that p38, MAPK, JNK, and AKT are required for vGCPR-induced HO-1

expression (data not shown). This is not surprising as vGCPR activates all these kinases (15, 24), and their requirement to activate the *ho-1* promoter has already been reported (4, 48, 49). MAPKs transactivate several AP-1 members and AKT activates NFκB, all transcription factors involved in the control of the *ho-1* promoter (2). While our preliminary data indicate the involvement of these molecular routes, the precise identification of the signaling pathways activated by vGCPR and of new transcription factors acting on the *ho-1* promoter draws a complex complicated picture that is the subject of current investigations.

vGPCR increases HO-1 expression in fibroblasts and endothelial cells, and this is a notable finding, as most cells are considered to express low or null amounts of the enzyme unless exposed to stress-triggering stimuli (50). Moreover, the fact that mouse tumors derived from vGPCR-expressing cells show high levels of HO-1 is consistently with the reported positive staining for HO-1 in KS biopsies (12). This interesting finding is in line with a recent study showing that as a result of the oncogenic activity of the BCR/Abl chimera, leukemic cells from patients with myeloid leukemia display elevated expression levels of HO-1 (50). Similarly, pancreatic cancer presents a higher index of mutated Ras (31) and HO-1 overexpression (32, 51). Although a direct correlation between Ras and HO-1 has not been studied, our preliminary results suggest that HO-1 is also partially required for activated Ras to induce transformation further supporting a possible more common role for HO-1 in tumorigenesis. Since HO-1 is expressed in various rapidly proliferating tumor cells, including adenocarcinoma, hepatoma, sarcoma, glioblastoma, melanoma, and squamous cells carcinoma (52), it is captivating to think that oncogene-dependent expression of HO-1 may be a common phenomenon occurring in several types of aberrant cell growth-associated malignancies.

The first indication of the requirement for HO-1 activity in the development of vGPCR-dependent cell transformation came from the observation that the HO-1 inhibitor SnPP did prevent vGPCR-transforming capability in cell culture models. Although SnPP can block both HO-1 and HO-2 activity, the fact that HO-2 expression is almost undetectable in NIH3T3 cells made us assume that the protoporphyrin was acting on the predominantly expressed HO-1 isoform. Still, to rule out secondary effects of SnPP, and taking into account that HO-1 activity depends mainly on its protein level, we speculated that blocking the expression of the enzyme should have the same effect as that of inhibiting its activity. Indeed, targeted knock-down of HO-1 mRNA with a specific shRNA also blocks vGPCR-induced focus formation (Fig. 3, *B* and *C*). The comparable results obtained with these two approaches confirmed the requirement for HO-1 in vGPCR-dependent transformation.

Considering that infection of endothelial cells by KSHV or by a vGCPR-carrying retrovirus induces the appearance of a spindle cell phenotype, typical of KS lesions (13, 18, 34, 35), we used murine endothelial cell lines to address the role of HO-1 in vGPCR-promoted cell growth. We observed that the sole overexpression of HO-1 was able to induce endothelial cell survival and proliferation to levels comparable with those induced by overexpression of vGPCR (Fig. 4, *B–E*). Furthermore, treatment of SVEC-vGPCR and SVEC-HA-HO-1 cells with SnPP reduced both annexin V staining and [^{3}H]thymidine incorporation (Fig. 4, *C–F*). These observations agreed with the postulated role for HO-1 as a central regulator of endothelial cell growth (3) and point out its participation on vGPCR-induced pro-survival/proliferative signaling. These outcomes are extensive to fibroblasts, as parallel experiments using the NIH3T3 derivatives, NIH-vGPCR and NIH-HO-1 cells, rendered nearly identical results. Interestingly, if both fibroblasts and endothelial cells were kept in serum-containing media, the effect of SnPP treatment was less pronounced (data not shown), and this would help explain why no apparent cell death was observed in the focus formation assay during 2–3 weeks of SnPP treatment, as cells were kept in 5% serum. However, it is worth mentioning that after a prolonged exposure to SnPP (5–6 weeks), cell detachment and mortality were higher than that of untreated cells (data not shown).

VEGF is one of the key factors involved in new blood vessel formation within tumors (39) and is ubiquitously found in KS lesions (53, 54). As such, it plays a central role in the pathogenesis of KS and in the angiogenic activity of vGPCR (16, 35). In this paper, we show that cells expressing HO-1 displayed VEGF mRNA levels similar to those found in vGPCR-expressing cells and that transient expression of HO-1 induces the activity of a *vegf* promoter-driven reporter (Fig. 5, *A* and *B*). More interesting is the fact that treating cells with SnPP or cotransfecting a HO-1-specific shRNA had a strong inhibitory effect on vGPCR-induced *vegf* promoter activity, which suggests that HO-1 is an important mediator in the pathway that connects the viral oncogene to VEGF (Fig. 5, *C* and *D*). In line with this observation, stable expression of VEGF in vGPCR-expressing cells (Fig. 5*E*) rescued the apoptotic phenotype induced by SnPP (Fig. 5*F*) indicating that indeed, HO-1 can be mediating vGPCR-induced cell survival by inducing the expression of VEGF. Although $CoCl_2$-induced hypoxia does not seem to require HO-1 to induce VEGF expression, angiogenic factors such as IL-6, for example, seem to require HO-1 enzymatic activity to induce VEGF (Fig. 6*A*). Our findings are analogous to a number of recent studies showing that angiogenic stimuli such as cytokines, prolactin, and the pGJ2 prostaglandin generated in the vasculature are able to induce HO-1 and VEGF expression. Notoriously, in all these cases, pretreatment with SnPP abolishes these effects, and knock-out of the HO-1 gene impaired the induction of VEGF by several stimuli, confirming a link between HO-1 and VEGF expresssion (42, 55, 56). It is known that HO-1 exerts anti-apoptotic effects through generation of heme degradation products, including CO, iron, and biliverdin (11), and the role of these molecules on VEGF synthesis and angiogenesis has been increasingly reported (3). We found that an 8-h exposure to $[Ru(CO)_3Cl_2]_2$ (a spontaneously CO-releasing molecule (57) that promotes angiogenesis (58)) induced a modest but significant increase in the activity of the *vegf* promoter in endothelial cells and fibroblasts (data not shown) as shown previously (29). The mechanisms by which CO induces VEFG secretion are rather complex and poorly understood. We have seen that $[Ru(CO)_3Cl_2]_2$ induces the MAPK p38α (data not shown) accordingly to other studies (59, 60). Coincidently, vGPCR-induced p38α phosphorylates and induces the transcriptional activity of Hif-1α, a hypoxia-inducible factor that regulates the expression of the *vegf* promoter (40). In addition, p38α regulates AP-1 transcriptional activity (61), and this transcription factor also controls vGPCR-driven *vegf* promoter activity (15, 24). Interestingly, very recent studies have shown that STAT3 is required by vGPCR to induce transformation (62) and by several other oncogenes to induce VEGF secretion (63). We have also found that $[Ru(CO)_3Cl_2]_2$ induces AKT (data not shown), and this kinase and p38α are required by CO to induce STAT3 and protect endothelial cells from apoptosis (64). Together, it is possible to speculate that HO-1, by means of its by-product CO, could control the activity of AKT and p38, and in turn, that of Hif-1α, AP-1, and STAT3, all transcription factors that can mediate vGPCR-induced VEGF expression. On the other hand, HO-1 also induces the release of iron from heme and its efflux from the cell, thus preventing apoptosis (65). As iron is the cofactor for prolyl hydoxylases, the enzymes that destabilize and target Hif1-α for ubiquitination, it can be hypothesized that HO-1-mediated iron extrusion leads to Hif-1α stabilization and consequent VEGF expression. The third by-product

released upon HO-1 activation is biliverdin, which is later converted to bilirubin by the biliverdin reductase (66). Although we observed a small increase in pVEGF-Luc activity upon 8-h bilirubin treatment of SVEC (data not shown), its effect on angiogenesis and VEGF secretion is less understood (3). Together, these conjectures evidence the complexity of the many genes and signal transduction pathways that can be activated upon increased HO-1 expression to result in deregulated cell survival and proliferation as a final outcome.

All of the above observations prompted us to ask whether HO-1 can be used as a molecular target in an *in vivo* model of vGPCR-induced tumorigenesis. We were greatly surprised by the fact that NIH-vGPCR cells in which HO-1 expression was knocked down by RNA interference were less potent than NIH-vGPCR cells to induce tumors when injected into the flank of nude mice, which verified that impairment of HO-1 expression affects vGPCR-transforming potential (Fig. 7*A*). Very recently and during the time our work was in progress, similar results have been shown in a model of pancreatic cancer where RNA interference of HO-1 led to pronounced growth inhibition of the pancreatic cancer cells and made tumor cells significantly more sensitive to radiotherapy and chemotherapy (32). Even more striking was the effect of the HO-1 inhibitor SnPP, as animals treated with this compound showed a remarkable reduction in vGPCR-induced tumor growth (Figs. 6*B* and 7*B*). Instead, animals treated with CoPP, a cobalt protoporphyrin that induces HO-1 expression and consequent activity, displayed larger tumors than vehicle-treated mice, confirming that HO-1 plays an important role in tumor growth control. Although both SnPP and CoPP induce HO-1 expression (Fig. 6*A*), only SnPP inhibits VEGF expression and tumor growth (Fig. 6, *A* and *B*). This correlates directly with the ability of SnPP, but not of CoPP, to act as a competitive inhibitor of HO-1, indicating that the activity of the enzyme plays a key role in vGPCR-induced tumor growth. Of note, vGPCR-induced tumors from vehicle-treated animals showed elevated HO-1 mRNA, protein expression, and activity levels. As expected, tumors from SnPP-treated animals displayed higher HO-1 mRNA and protein levels because of SnPP acting at the level of HO-1 expression (30). Instead, they had basically null HO-1 activity levels (Fig. 8, *A–C*), confirming that the protoporphytin reached the tumor tissue and inhibited HO-1 activity in our model system. The HO-1 activity detected in vehicle- and SnPP-treated tumors correlated directly with VEFG-A but not VEGF-C mRNA levels, in line with the observations made in cultured cells (Figs. 5*A* and 8*B*). Both tumors expressed equal levels of vGPCR, but VEGF-A mRNA levels were strongly reduced in SnPP-treated tumors. These results indicate that SnPP did not induce a delayed tumor growth by affecting vGPCR levels but rather blocked the expression of one of the fundamental genes required for vGPCR oncogenic activity (Fig. 8*C*). The capacity of HO-1 to induce VEGF expression and cell growth *in vivo* has also been observed in rat placenta, where transduction with adenoviral human HO-1 resulted in increased expression of vascular endothelial growth factor and pup size, whereas inhibition of the enzyme by metalloporphyrins decreased fetal growth (67). Noteworthy, SnPP has been extensively used *in vivo* to treat several pathologies including murine collagen-induced arthritis (68) and hyperbilirubinemia in rats, monkeys, and humans (69–71). A recent clinical trial with newborns shows that the inhibitor can be administered at any time point in the progression of postnatal hyperbilirubinemia to rapidly and predictably block heme degradation to bilirubin and prevent severe jaundice without significant short or long term side effects detected in treated infants (71). Taking into account the lack of apparent secondary effects of prolonged SnPP treatment and its potent inhibitory effect on tumor growth, SnPP emerges as an appealing antitumor candidate drug. Similary, another HO-1 inhibitor, zinc protoporphyrin (ZnPP), and its water-soluble pegylated form (PEG-ZnPP), have been recently found to act as antineoplastic agents in rats and mice bearing tumors derived from hepatoma and human colon cancer cells, respectively (52, 72).

In conclusion, our data show for the first time that vGPCR induces HO-1 and that genetic or chemical inhibition of the enzyme results in a clear reduction of vGPCR-induced cell transformation and tumor growth. Considering that HO-1 is overexpressed in human KS lesions (12), the targeted inhibition of intratumoral HO-1 activity by metalloporphyrins as a new anticancer tactic in the treatment of KS may be of potential clinical interest and warrants further investigation.

Acknowledgments—We thank Manuel Izquierdo and Carla Mazzeo for their advice and help with microscopy, Mario Chiariello for kindly revising the manuscript, J. S. Gutkind for the gift of the pCEFL-VEGF plasmid, and Jorge Boczkowski for his help with the HO-1 activity assay.

REFERENCES

1. Maines, M. D., and Gibbs, P. E. (2005) *Biochem. Biophys. Res. Commun.* **338,** 568–577
2. Alam, J., Igarashi, K., Immenschuh, S., Shibahara, S., and Tyrrell, R. M. (2004) *Antioxid. Redox Signal.* **6,** 924–933
3. Dulak, J., Loboda, A., Zagorska, A., and Jozkowicz, A. (2004) *Antioxid. Redox Signal.* **6,** 858–866
4. Salinas, M., Diaz, R., Abraham, N. G., Ruiz de Galarreta, C. M., and Cuadrado, A. (2003) *J. Biol. Chem.* **278,** 13898–13904
5. Martin, D., Rojo, A. I., Salinas, M., Diaz, R., Gallardo, G., Alam, J., De Galarreta, C. M., and Cuadrado, A. (2004) *J. Biol. Chem.* **279,** 8919–8929
6. Malaguarnera, L., Imbesi, R. M., Scuto, A., D'Amico, F., Licata, F., Messina, A., and Sanfilippo, S. (2004) *J. Cell. Biochem.* **93,** 197–206
7. Lam, C. W., Getting, S. J., and Perretti, M. (2005) *J. Immunol.* **174,** 2297–2304
8. Kiemer, A. K., Bildner, N., Weber, N. C., and Vollmar, A. M. (2003) *Endocrinology* **144,** 802–812
9. Poss, K. D., and Tonegawa, S. (1997) *Proc. Natl. Acad. Sci. U. S. A.* **94,** 10925–10930
10. Amersi, F., Buelow, R., Kato, H., Ke, B., Coito, A. J., Shen, X. D., Zhao, D., Zaky, J., Melinek, J., Lassman, C. R., Kolls, J. K., Alam, J., Ritter, T., Volk, H. D., Farmer, D. G., Ghobrial, R. M., Busuttil, R. W., and Kupiec-Weglinski, J. W. (1999) *J. Clin. Invest.* **104,** 1631–1639
11. Otterbein, L. E., Soares, M. P., Yamashita, K., and Bach, F. H. (2003) *Trends Immunol.* **24,** 449–455
12. McAllister, S. C., Hansen, S. G., Ruhl, R. A., Raggo, C. M., DeFilippis, V. R., Greenspan, D., Fruh, K., and Moses, A. V. (2004) *Blood* **103,** 3465–3473
13. Flore, O., Rafii, S., Ely, S., O'Leary, J. J., Hyjek, E. M., and Cesarman, E. (1998) *Nature* **394,** 588–592
14. Nicholas, J. (2003) *J. Biomed. Sci.* **10,** 475–489
15. Arvanitakis, L., Geras-Raaka, E., Varma, A., Gershengorn, M. C., and Cesarman, E. (1997) *Nature* **385,** 347–350
16. Bais, C., Santomasso, B., Coso, O., Arvanitakis, L., Raaka, E. G., Gutkind, J. S., Asch, A. S., Cesarman, E., Gershengorn, M. C., and Mesri, E. A. (1998) *Nature* **391,** 86–89
17. Yang, T. Y., Chen, S. C., Leach, M. W., Manfra, D., Homey, B., Wiekowski, M., Sullivan, L., Jenh, C. H., Narula, S. K., Chensue, S. W., and Lira, S. A. (2000) *J. Exp. Med.* **191,** 445–454
18. Montaner, S., Sodhi, A., Molinolo, A., Bugge, T. H., Sawai, E. T., He, Y., Li, Y., Ray, P. E., and Gutkind, J. S. (2003) *Cancer Cell* **3,** 23–36
19. Jensen, K. K., Manfra, D. J., Grisotto, M. G., Martin, A. P., Vassileva, G., Kelley, K., Schwartz, T. W., and Lira, S. A. (2005) *J. Immunol.* **174,** 3686–3694
20. Goldhar, A. S., Vonderhaar, B. K., Trott, J. F., and Hovey, R. C. (2005) *Mol. Cell. Endocrinol.* **232,** 9–19
21. Marinissen, M. J., Chiariello, M., Tanos, T., Bernard, O., Narumiya, S., and Gutkind, J. S. (2004) *Mol. Cell* **14,** 29–41
22. Marinissen, M. J., Servitja, J. M., Offermanns, S., Simon, M. I., and Gutkind, J. S. (2003) *J. Biol. Chem.* **278,** 46814–46825
23. Abraham, N. G., Lavrovsky, Y., Schwartzman, M. L., Stoltz, R. A., Levere, R. D., Gerritsen, M. E., Shibahara, S., and Kappas, A. (1995) *Proc. Natl. Acad. Sci. U. S. A.* **92,** 6798–6802
24. Montaner, S., Sodhi, A., Servitja, J. M., Ramsdell, A. K., Barac, A., Sawai, E. T., and Gutkind, J. S. (2004) *Blood* **104,** 2903–2911
25. Gershengorn, M. C., Geras-Raaka, E., Varma, A., and Clark-Lewis, I. (1998) *J. Clin. Invest.* **102,** 1469–1472
26. Brouard, S., Otterbein, L. E., Anrather, J., Tobiasch, E., Bach, F. H., Choi, A. M., and Soares, M. P. (2000) *J. Exp. Med.* **192,** 1015–1026

27. Yoshinaga, T., Sassa, S., and Kappas, A. (1982) *J. Biol. Chem.* **257,** 7778–7785
28. Anderson, K. E., Simionatto, C. S., Drummond, G. S., and Kappas, A. (1984) *J. Pharmacol. Exp. Ther.* **228,** 327–333
29. Jozkowicz, A., Huk, I., Nigisch, A., Weigel, G., Dietrich, W., Motterlini, R., and Dulak, J. (2003) *Antioxid. Redox Signal.* **5,** 155–162
30. Sardana, M. K., and Kappas, A. (1987) *Proc. Natl. Acad. Sci. U. S. A.* **84,** 2464–2468
31. Forrester, K., Almoguera, C., Han, K., Grizzle, W. E., and Perucho, M. (1987) *Nature* **327,** 298–303
32. Berberat, P. O., Dambrauskas, Z., Gulbinas, A., Giese, T., Giese, N., Kunzli, B., Autschbach, F., Meuer, S., Buchler, M. W., and Friess, H. (2005) *Clin. Cancer Res.* **11,** 3790–3798
33. Miralem, T., Hu, Z., Torno, M. D., Lelli, K. M., and Maines, M. D. (2005) *J. Biol. Chem.* **280,** 17084–17092
34. Lagunoff, M., Bechtel, J., Venetsanakos, E., Roy, A. M., Abbey, N., Herndier, B., McMahon, M., and Ganem, D. (2002) *J. Virol.* **76,** 2440–2448
35. Bais, C., Van Geelen, A., Eroles, P., Mutlu, A., Chiozzini, C., Dias, S., Silverstein, R. L., Rafii, S., and Mesri, E. A. (2003) *Cancer Cell* **3,** 131–143
36. Deramaudt, B. M., Braunstein, S., Remy, P., and Abraham, N. G. (1998) *J. Cell Biochem.* **68,** 121–127
37. Kushida, T., Quan, S., Yang, L., Ikehara, S., Kappas, A., and Abraham, N. G. (2002) *Biochem. Biophys. Res. Commun.* **291,** 68–75
38. Yachie, A., Niida, Y., Wada, T., Igarashi, N., Kaneda, H., Toma, T., Ohta, K., Kasahara, Y., and Koizumi, S. (1999) *J. Clin. Invest.* **103,** 129–135
39. Ferrara, N. (2002) *Nat. Rev. Cancer* **2,** 795–803
40. Sodhi, A., Montaner, S., Patel, V., Zohar, M., Bais, C., Mesri, E. A., and Gutkind, J. S. (2000) *Cancer Res.* **60,** 4873–4880
41. Guo, H. G., Sadowska, M., Reid, W., Tschachler, E., Hayward, G., and Reitz, M. (2003) *J. Virol.* **77,** 2631–2639
42. Cisowski, J., Loboda, A., Jozkowicz, A., Chen, S., Agarwal, A., and Dulak, J. (2005) *Biochem. Biophys. Res. Commun.* **326,** 670–676
43. Tang, R. F., Wang, S. X., Zhang, F. R., Peng, L., Wang, S. X., Xiao, Y., and Zhang, M. (2005) *Hepatobiliary Pancreat. Dis. Int.* **4,** 460–463
44. Loboda, A., Jazwa, A., Wegiel, B., Jozkowicz, A., and Dulak, J. (2005) *Cell Mol. Biol.* (*Noisy-le-grand*) **51,** 347–355
45. Sacerdoti, D., Colombrita, C., Ghattas, M. H., Ismaeil, E. F., Scapagnini, G., Bolognesi, M., Li Volti, G., and Abraham, N. G. (2005) *Cell Mol. Biol.* (*Noisy-le-grand*) **51,** 363–370
46. Reeve, V. E., and Tyrrell, R. M. (1999) *Proc. Natl. Acad. Sci. U. S. A.* **96,** 9317–9321
47. Fang, J., Sawa, T., Akaike, T., Akuta, T., Sahoo, S. K., Khaled, G., Hamada, A., and Maeda, H. (2003) *Cancer Res.* **63,** 3567–3574
48. Alvarez-Maqueda, M., El Bekay, R., Alba, G., Monteseirin, J., Chacon, P., Vega, A., Martin-Nieto, J., Bedoya, F. J., Pintado, E., and Sobrino, F. (2004) *J. Biol. Chem.* **279,** 21929–21937
49. Lee, T. S., Chang, C. C., Zhu, Y., and Shyy, J. Y. (2004) *Circulation* **110,** 1296–1302
50. Mayerhofer, M., Florian, S., Krauth, M. T., Aichberger, K. J., Bilban, M., Marculescu, R., Printz, D., Fritsch, G., Wagner, O., Selzer, E., Sperr, W. R., Valent, P., and Sillaber, C. (2004) *Cancer Res.* **64,** 3148–3154
51. Sunamura, M., Duda, D. G., Ghattas, M. H., Lozonschi, L., Motoi, F., Yamauchi, J., Matsuno, S., Shibahara, S., and Abraham, N. G. (2003) *Angiogenesis* **6,** 15–24
52. Fang, J., Akaike, T., and Maeda, H. (2004) *Apoptosis* **9,** 27–35
53. Cornali, E., Zietz, C., Benelli, R., Weninger, W., Masiello, L., Breier, G., Tschachler, E., Albini, A., and Sturzl, M. (1996) *Am. J. Pathol.* **149,** 1851–1869
54. Masood, R., Cai, J., Zheng, T., Smith, D. L., Naidu, Y., and Gill, P. S. (1997) *Proc. Natl. Acad. Sci. U. S. A.* **94,** 979–984
55. Jozkowicz, A., Huk, I., Nigisch, A., Weigel, G., Weidinger, F., and Dulak, J. (2002) *Antioxid. Redox Signal.* **4,** 577–585
56. Dulak, J., Jozkowicz, A., Foresti, R., Kasza, A., Frick, M., Huk, I., Green, C. J., Pachinger, O., Weidinger, F., and Motterlini, R. (2002) *Antioxid. Redox Signal.* **4,** 229–240
57. Motterlini, R., Mann, B. E., Johnson, T. R., Clark, J. E., Foresti, R., and Green, C. J. (2003) *Curr. Pharm. Des.* **9,** 2525–2539
58. Li Volti, G., Sacerdoti, D., Sangras, B., Vanella, A., Mezentsev, A., Scapagnini, G., Falck, J. R., and Abraham, N. G. (2005) *Antioxid. Redox Signal.* **7,** 704–710
59. Otterbein, L. E., Bach, F. H., Alam, J., Soares, M., Tao Lu, H., Wysk, M., Davis, R. J., Flavell, R. A., and Choi, A. M. (2000) *Nat. Med.* **6,** 422–428
60. Zhang, X., Shan, P., Otterbein, L. E., Alam, J., Flavell, R. A., Davis, R. J., Choi, A. M., and Lee, P. J. (2003) *J. Biol. Chem.* **278,** 1248–1258
61. Tanos, T., Marinissen, M. J., Leskow, F. C., Hochbaum, D., Martinetto, H., Gutkind, J. S., and Coso, O. A. (2005) *J. Biol. Chem.* **280,** 18842–18852
62. Burger, M., Hartmann, T., Burger, J. A., and Schraufstatter, I. (2005) *Oncogene* **24,** 2067–2075
63. Xu, Q., Briggs, J., Park, S., Niu, G., Kortylewski, M., Zhang, S., Gritsko, T., Turkson, J., Kay, H., Semenza, G. L., Cheng, J. Q., Jove, R., and Yu, H. (2005) *Oncogene* **24,** 5552–5560
64. Zhang, X., Shan, P., Alam, J., Fu, X. Y., and Lee, P. J. (2005) *J. Biol. Chem.* **280,** 8714–8721
65. Ferris, C. D., Jaffrey, S. R., Sawa, A., Takahashi, M., Brady, S. D., Barrow, R. K., Tysoe, S. A., Wolosker, H., Baranano, D. E., Dore, S., Poss, K. D., and Snyder, S. H. (1999) *Nat. Cell Biol.* **1,** 152–157
66. Baranano, D. E., Rao, M., Ferris, C. D., and Snyder, S. H. (2002) *Proc. Natl. Acad. Sci. U. S. A.* **99,** 16093–16098
67. Kreiser, D., Nguyen, X., Wong, R., Seidman, D., Stevenson, D., Quan, S., Abraham, N., and Dennery, P. A. (2002) *Lab. Invest.* **82,** 687–692
68. Devesa, I., Ferrandiz, M. L., Terencio, M. C., Joosten, L. A., van den Berg, W. B., and Alcaraz, M. J. (2005) *Arthritis Rheum.* **52,** 3230–3238
69. Cornelius, C. E., and Rodgers, P. A. (1984) *Pediatr. Res.* **18,** 728–730
70. Kappas, A., Drummond, G. S., and Valaes, T. (2001) *Pediatrics* **108,** 25–30
71. Drummond, G. S., and Kappas, A. (2004) *Semin. Perinatol.* **28,** 365–368
72. Doi, K., Akaike, T., Fujii, S., Tanaka, S., Ikebe, N., Beppu, T., Shibahara, S., Ogawa, M., and Maeda, H. (1999) *Br. J. Cancer* **80,** 1945–1954

Mechanisms of Signal Transduction:

Inhibition of Heme Oxygenase-1 Interferes with the Transforming Activity of the Kaposi Sarcoma Herpesvirusencoded G Protein-coupled Receptor

Maria Julia Marinissen, Tamara Tanos, Marta Bolós, Maria Rosa de Sagarra, Omar A. Coso and Antonio Cuadrado

J. Biol. Chem. 2006, 281:11332-11346.
doi: 10.1074/jbc.M512199200 originally published online February 13, 2006